bioRxiv preprint doi: https://doi.org/10.1101/843870; this version posted November 17, 2019. The copyright holder for this preprint (which was not certified by peer review) is the author/funder, who has granted bioRxiv a license to display the preprint in perpetuity. It is made available under aCC-BY-ND 4.0 International license.

A new *Brachiaria* reference genome and its application in identifying genes associated with natural variation in tolerance to acidic soil conditions among *Brachiaria* grasses

Margaret Worthington[1#], Juan Guillermo Perez[1], Saule Mussurova[2], Alexander Silva-Cordoba[1], Valheria Castiblanco[1], Charlotte Jones[3], Narcis Fernandez-Fuentes[3], Leif Skot[3], Sarah Dyer[2&], Joe Tohme[1], Federica Di Palma[2], Jacobo Arango[1], Ian Armstead[3], Jose J De Vega[2*]

1. International Center for Tropical Agriculture (CIAT), A.A. 6713, Cali, Colombia.
2. Earlham Institute, Norwich Research Park, Norwich, NR4 7UZ, UK.
3. Institute of Biological, Environmental and Rural Sciences (IBERS), Aberystwyth University, Aberystwyth, UK.

Present address: Department of Horticulture, University of Arkansas, 306 Plant Sciences Bldg, Fayetteville, AR, 72701, USA.
& Present address: NIAB, Huntingdon Road, Cambridge, CB3 0LE, UK.

* Correspondence to jose.devega@earlham.ac.uk; Earlham Institute, Norwich Research Park, Norwich, NR4 7UZ, UK.

bioRxiv preprint doi: https://doi.org/10.1101/843870; this version posted November 17, 2019. The copyright holder for this preprint (which was not certified by peer review) is the author/funder, who has granted bioRxiv a license to display the preprint in perpetuity. It is made available under aCC-BY-ND 4.0 International license.

ABSTRACT

Toxic concentrations of aluminium cations and low phosphorus availability are the main yield-limiting factors in acidic soils, which represent half of the potentially available arable land. *Brachiaria* grasses, which are commonly sown as a forage in the tropics because of their resilience and low demand for nutrients, have a greater tolerance to high concentrations of aluminium cations than most other grass crops. In this work, we explored the natural variation in tolerance to aluminium cations between high and low tolerant *Brachiaria* species and characterised their transcriptional differences during stress. We also identified three QTLs associated with root vigour during aluminium cation stress in their hybrid progeny. By integrating these results with a new *Brachiaria* reference genome, we have identified genes associated with aluminium cation tolerance in *Brachiaria*. We observed differential expression of response signalling, cell wall composition and vesicle transport genes homologous to aluminium-induced proteins involved in limiting uptake or localizing toxic agents. However, there was limited regulation of malate transporters, which are detected during Al^{3+} stress in other grasses. Contrasting regulation during Al^{3+} stress of numerous genes involved in RNA translation suggests variations in response timing may be associated with the differences in tolerance to aluminium cations among *Brachiaria* species.

INTRODUCTION

Acidic soils constitute circa 30 % of the world's total land area and 50 % of the potentially available arable land (Von Uexküll and Mutert 1995). Acidic soils are particularly predominant in two regions in the world, a northern "temperate belt" and a southern "subtropical belt" (Hede, Skovmand, and Lopez Cesati 2001). Therefore, a broad range of vegetable, cereal and forage crops can be yield-limited in these conditions. While low soil pH *per se* can have an inhibitory effect on plant growth for non-adapted species, the adverse effects of soil acidity are mostly associated with several mineral toxicities and deficiencies, particularly increased concentrations of soluble forms of manganese, iron and aluminium, and reduced levels of available forms of phosphorus, calcium, magnesium and potassium. Among these, lower phosphorus solubility and aluminium toxicity are considered the main limiting factors on productivity (Eswaran, Reich, and Beinroth 1997). As soil pH decreases below 5, aluminium becomes soluble as the aluminium trivalent cation (Al^{3+}), a form highly toxic to plants. Soluble Al^{3+} effect on root apices results in diminished ion and water uptake.

bioRxiv preprint doi: https://doi.org/10.1101/843870; this version posted November 17, 2019. The copyright holder for this preprint (which was not certified by peer review) is the author/funder, who has granted bioRxiv a license to display the preprint in perpetuity. It is made available under aCC-BY-ND 4.0 International license.

Although acid soils can be conditioned for improved agricultural use through the addition of lime (quicklime, calcium oxide or slag, calcium silicate, etc.), this agronomic practice is undesirable due to the broader implications for other fauna, flora and the soil microbial populations and, in general, the best long-term strategy is a combination of agronomic practices and growing tolerant cultivars. Natural variation in aluminium tolerance has been identified for a number of crops with rice being the most aluminium-tolerant among the food staples (Rao et al. 2016). However, all *Brachiaria* species show greater tolerance to Al^{3+} toxicity than most other grass crops, including maize, rice or wheat (Kochian et al. 2015).

Brachiaria (Trin.) Griseb. (syn. *Urochloa* P.Beauv.) grasses are native to East Africa and are widely sown as a forage to feed ruminants across the tropics, particularly in areas with marginal soils. *Brachiaria* has a set of desirable genetic characteristics linked to drought and waterlogging tolerance, poor and acidic soils tolerance, and resistance to major diseases. However, *Brachiaria* resilience is principally a result of low demand for soil nutrients (Pizarro et al. 2013; Worthington and Miles 2015). As a consequence, toxic cation levels (and not reduced levels of mineral solutes) are the limiting factors on *Brachiaria* species productivity in acidic soil conditions.

Al^{3+} tolerance has been established to be a multigenic trait, though major genes can also be important (Ryan et al. 2009; Kochian et al. 2015). The incomplete transfer of tolerance from parents to near-isogenic lines in sorghum (Melo et al. 2013), maize (Guimaraes et al. 2014), and wheat (Johnson, Carver, and Baligar 1997; Tang et al. 2002) supports polygenic inheritance of Al^{3+} tolerance. While a single locus in barley (*Alp*) confers significant tolerance to Al^{3+} in the elite material (Minella and Sorrells 1992), different loci appear to play an essential role in Asian landraces (Caniato et al. 2007).

Al^{3+} tolerance mechanisms are classified as external and internal tolerance mechanisms (Furlan et al. 2018; Kochian et al. 2015). In the first group, plants prevent Al^{3+} uptake by raising the pH in the rhizosphere by H^+ influx or forming binding complexes by exudation of citrate, malate and oxalate. In the second group, Al^{3+} is absorbed and localized to cell organelles or the apoplast. In tolerant rice variety Nipponbare, both exclusion mechanisms and internal detoxification are important in withstanding toxicity, while primarily internal detoxification occurs in sensitive rice variety Modan (Roselló et al. 2015).

Little is known about the genetic basis of the Al^{3+} tolerance in *Brachiaria*. Nevertheless, screening experiments have evidenced different but consistent aluminium tolerance among *Brachiaria* species and cultivars, which indicates the genetic basis of the trait (Arroyave et al.

bioRxiv preprint doi: https://doi.org/10.1101/843870; this version posted November 17, 2019. The copyright holder for this preprint (which was not certified by peer review) is the author/funder, who has granted bioRxiv a license to display the preprint in perpetuity. It is made available under aCC-BY-ND 4.0 International license.

2013). The three most important commercial species, *Brachiaria brizantha* (A.Rich.) Stapf., *B. decumbens* Stapf., and *B. humidicola* (Rendle) Schweick exist primarily as apomicts with varying levels of polyploidy (Valle and Savidan 1996). The sexual species *B. ruziziensis* (Germ.&C.M.Evrard) is also used in breeding. *B. decumbens* is significantly more tolerant to Al^{3+} than *B. ruziziensis* (Arroyave et al. 2011; Bitencourt et al. 2011).

Brachiaria is one of the most widely used and promising forages in the American and African tropics and for the potential of this species to be realised, it is important that varieties are tailored to the particular demands of each environment in which it is grown (Bailey-Serres et al. 2019). One of the tools available for identifying locally adapted variation is molecular characterisation. However, underpinning genomic resources are costly to produce and so often limited for 'orphan' crop species such as *Brachiaria*. To this end, the work presented here has focused on developing a) genomic resources for *Brachiaria* and b) the application of these in developing a better understanding of the molecular basis of a key trait affecting Brachiaria productivity, namely Al^{3+} tolerance.

METHODS

Plant materials and phenotyping

The mapping population used in this work consisted of 169 genotypes of F1 progeny from a cross between the autopolyploid BRX 44-02 (*B. ruziziensis*) and the segmental allopolyploid CIAT 606 (*B. decumbens*). This population was generated initially to identify markers linked to apomixis (Worthington et al. 2016). Accessions were phenotyped at CIAT in Cali, Colombia, and consisted of six cycles where plants were grown for 20 days in hydroponic solutions with 0 and 200 µM $AlCl^3$. Measurements of cumulative root length (RL), root biomass (RB), and root tip diameter (RD) were taken at the end of each cycle and transformed to meet the assumption of normality; RL and RB were square-root transformed and RD was natural log-transformed. The PROC MIXED method in SAS was used to fit a mixed effect model. Genotypic BLUPs were calculated from stress and control measurements individually, back transformed BLUP in the natural scale were obtained by dividing stress and control values for each trait.

Genome sequencing, assembly and annotation

bioRxiv preprint doi: https://doi.org/10.1101/843870; this version posted November 17, 2019. The copyright holder for this preprint (which was not certified by peer review) is the author/funder, who has granted bioRxiv a license to display the preprint in perpetuity. It is made available under aCC-BY-ND 4.0 International license.

B. ruziziensis genotype 26162 (2n = 2x = 18) was the source of genomic DNA. Two paired-end libraries were created and sequenced in Illumina HiSeq 2500 machines in rapid run mode by the Earlham Institute (approx. 70X) and the Yale Center for Genome Analysis (approx. 30X) following the manufacturer's protocol. Additionally, a Nextera mate-pair (MP) library with insert length 7 Kb was sequenced to improve the scaffolding. Read quality was assessed, and contaminants and adaptors removed. Illumina Nextera MP reads were required to include a fragment of the adaptor to be used in the following steps (Leggett, Clavijo, et al. 2013). The pair-end shotgun libraries were assembled and later scaffolded using the mate-pairs library using Platanus v1.2.117, which is optimized for heterozygous genomes (Kajitani et al. 2014). We did not use Platanus' gap-closing step. Approximately 1 million Pacbio reads from this same genotype were generated in a PacBio RSII sequencer, and used for gap filling using PBJelly v.15.8.24 (English et al. 2012). Scaffolds shorter than 1 Kbp were filtered out. We used 31mer spectra analysis to compare the assemblies produced by different pipelines, as well as our final assembly with the intermediary assemblies from preceding steps. A K-mer spectrum is a representation of how many fixed-length words or K-mers (y-axis) appear a certain number of times or coverage (x-axis). The K-mer counting was performed with KAT (Mapleson et al. 2016). The completeness of the assembly was checked with BUSCO (Simão et al. 2015).

Repetitive and low complexity regions of the scaffolds were masked using RepeatMasker (Tarailo-Graovac and Chen 2009) based on self-alignments and homology with the RepBase public database and specific databases built with RepeatModeler (Smit and Hubley 2008). LTR retrotransposons were detected by LTRharvest (Ellinghaus, Kurtz, and Willhoeft 2008) and classified with RepeatClassifier. The 5′ and 3′ ends of each LTR were aligned to each other with MUSCLE (Edgar 2004) and used to calculate the nucleotide divergence rate with the Kimura-2 parameter using MEGA6 (Tamura et al. 2013). The insertion time was estimated by assuming an average substitution rate of 1.3×10^{-8} (Schmutz et al. 2014)

Our annotation pipeline (De Vega et al. 2015) uses four sources of evidence. (a) *De novo* and genome-guided *ab initio* transcripts deduced from RNA-Seq reads from the *B. ruziziensis* genotype assembled with Trinity (Grabherr et al. 2011) and Tophat and Cufflinks (Trapnell et al. 2012), (b) gene models predicted by Augustus (Stanke et al. 2006), (c) homology-based alignments of transcripts and proteins from four close species with Exonerate and GMAP (Wu et al. 2016), and (d) the repeats annotation. Finally, MIKADO (Venturini et al. 2018) built the gene models to be compatible with this previous information. Proteins were compared with the NCBI non-redundant proteins and EBI's InterPro

bioRxiv preprint doi: https://doi.org/10.1101/843870; this version posted November 17, 2019. The copyright holder for this preprint (which was not certified by peer review) is the author/funder, who has granted bioRxiv a license to display the preprint in perpetuity. It is made available under aCC-BY-ND 4.0 International license.

databases and the results were imported into Blast2GO (Conesa et al. 2005) to annotate the GO and GO slim terms, enzymatic protein codes and KEGG pathways. Proteins were also functionally annotated with the GO terms of any significant orthologous protein in the eggNOG database (Powell et al. 2014), using the eggNOG-mapper pipeline (Huerta-Cepas et al. 2017).

Population genotyping and genetic map construction

Genotyping-by-sequencing libraries were prepared and sequenced for the 169 F1 progenies and the two parents as described in Worthington et al 2016. Reads were demultiplexed according to the forward and reverse barcodes used during library preparation with FastGBS (Torkamaneh et al. 2017) and adaptors and enzymatic motifs removed with Cutadapt (Martin 2011). Reads were aligned to the genome using BWA MEM (Li 2013). SNP calling was done for each sample with GATK's Haplotycaller (Van der Auwera et al. 2013) without the duplicated read filter (-drf DuplicateRead) and recalled for the population with GATK's GenotypeGVCFs, in both tools with "--ploidy 4". We changed to *missing call* any homozygous SNP supported by less than 12 reads, and any SNP supported by less than three reads. We removed any site not called in a progenitor or more than 20 % of the progeny. Markers that were heterozygous in only one parent and had a segregation ratio of a heterozygote to homozygote progeny of approximately 2:1 (between 0.5 and 1.75) were classified as single-dose allele (SDA) markers and used in the linkage map construction. Separated genetic linkage maps of BRX 44-02 and CIAT 606 were constructed in JoinMap v5; downstream QTL analysis used the *B. ruziziensis* BRX 44-02 map.

RNA-seq sequencing and analysis

The tolerance experiment in the greenhouse was fully replicated once. RNA extraction from each root and leaf sample was performed with RNeasy Plant Mini kit (Qiagen, CA, USA) and sent to the sequencing service provider where Illumina RNA-seq libraries were prepared and sequenced using the HiSeq 2500 platform. Sixteen libraries were independently generated and sequenced (two tissues, from two species, in two conditions, in two replicates). Contaminations in the raw data were discarded with Kontaminant (Leggett, Ramirez-Gonzalez, et al. 2013) against a database of common virus, bacteria and fungi. Adaptors were removed with Cutadapt (Martin 2011) and quality checked with FastQC (Andrews 2017). Reads were mapped to the genome using STAR (Dobin et al. 2013) and the gene models annotation for guidance. Counts were estimated with Stringtie (Pertea et al. 2015). We used DEseq v2 (Love, Huber, and Anders 2014) for analysing differential expression,

bioRxiv preprint doi: https://doi.org/10.1101/843870; this version posted November 17, 2019. The copyright holder for this preprint (which was not certified by peer review) is the author/funder, who has granted bioRxiv a license to display the preprint in perpetuity. It is made available under aCC-BY-ND 4.0 International license.

which takes as input a matrix of read counts mapped to each gene. Enriched GO terms and other categories in each group of differentially expressed genes were identified in R using TOPGO (Alexa and Rahnenfuhrer 2010) using a Fisher's test (FDR<0.05) and the "weight01" algorithm. The relation among GO terms was plotted in R using ggplot (Wickham and Chang 2008).

Comparative genomics

Syntenic blocks between *B. ruziziensis* and *S. italica* whole genomes were identified with Minimap (Li 2016), and plotted with D-GENIES (Cabanettes and Klopp 2018). Previously, we had filtered out any scaffolds shorter than 10Kbp that did not contain any gene. The assembly was anchored in *S. italica* by assigning each scaffold to the chromosome position where it had the longest alignment chain after combining proximal alignments. For clustering, proteins from five related species were assigned to eggNOG orthologous groups as before. A phylogenetic tree based on these data was built with MUSCLE, as before, by aligning the orthologous proteins from two species at a time, filtering sets with 1:1 ratios and, finally, estimating the nucleotide divergence rate using MEGA v6, as before.

RESULTS

Root morphology in *Brachiaria* species in different aluminium cation concentrations

We demonstrated the superior Al^{3+} tolerance of *B. decumbens* accession CIAT 606 compared with *B. ruziziensis* accession BRX 44-02 (Fig. 1). The root morphology in the *B. decumbens* accession was less affected than in the *B. ruziziensis* accessions after growing for 20 days in control and high (200 µM) Al^{3+} concentration hydroponic solutions. Under stress conditions, the roots of *B. decumbens* were over three times as long and had twice the biomass of *B. ruziziensis.* However, the root top diameter increased in stress conditions in a similar ratio in both species (Suppl. Table 1).

A population of 169 interspecific tetraploid progeny was obtained by crossing aluminium-tolerant *B. decumbens* accession CIAT 606 and aluminium-sensitive *B. ruziziensis* accession BRX 44-02. The interspecific progeny showed variation in cumulative root length (RL), root biomass (RB), and root tip diameter (RD) (Fig 2; Suppl. File 1). We obtained

bioRxiv preprint doi: https://doi.org/10.1101/843870; this version posted November 17, 2019. The copyright holder for this preprint (which was not certified by peer review) is the author/funder, who has granted bioRxiv a license to display the preprint in perpetuity. It is made available under aCC-BY-ND 4.0 International license.

243 highly significant ($p < 0.001$) genotypic differences in stress/control, control and stress
244 conditions for the three traits (RL, RB and RD).
245
246
247 **Assembly and annotation of a *Brachiaria* reference genome**
248
249 We selected the *B. ruziziensis* genotype CIAT 26162 (2n = 2x = 18) as the source of
250 genomic DNA. This is a semi-erect diploid accession from Burundi (-3.1167, 30.1333) that
251 was chromosome-doubled with colchicine to produce the autotetraploid *B. ruziziensis* BRX
252 44-02, one of the progenitors of the interspecific mapping population analysed. The ploidy of
253 CIAT 26162 has recently been verified by cytogenetics (*P. Tomaszewska, personal comm.*).
254 A whole-genome was assembled (WGS) using Platanus v.1.2.4 (Kajitani et al. 2014), from
255 Illumina paired-end and Nextera mate-pair reads with a coverage of approximately 100X and
256 7X, respectively (Suppl. Table 2). Platanus outperformed the contiguity results obtained with
257 other pipelines. Although the combination of ABySS for the contigs assembly and SOAP2 for
258 the scaffolding resulted in a larger assembly, a kmer frequency analysis (Mapleson et al.
259 2016) evidenced that the additional content was repeated under collapsed heterozygosity
260 that Platanus had purged (Suppl. Fig. 1). The assembly was followed by a gap-filling step
261 using approximately 1 million Pacbio reads with an average length of 4.8 Kbp, which
262 resulted in a reduced percentage of ambiguous nucleotides (Ns) from 17.45 % to 11.39 %.
263 We finally discarded all the sequences under 1 Kbp to produce the reference genome we
264 used for the downstream analysis (Table 1). To assess the completeness of the assembly,
265 we verified that 1,345 (93.4 %) of the 1,440 BUSCO orthologous genes (Simão et al. 2015)
266 were present in the assembly; 1,216 of which were completed and in a single copy, 32 were
267 duplicated, and 97 were fragmented. This WGS assembly is deposited in SRA with the
268 accession number GCA_003016355. The raw reads are deposited in the Bioproject
269 PRJNA437375.
270
271 The repeat content (Suppl. Table 3) was 51 % of the total genome (656,355,643 bp, after
272 excluding Ns), which is close to the 46 % repeat content in *Setaria italica* (L.) P. Beauv
273 (foxtail millet) (Zhang et al. 2012). We found a large number of Gypsy and Copia long
274 terminal repeats (LTRs), which represent 24 % and 9.5 % of the total genome excluding Ns.
275 These transposons and proportions are also very similar to those observed in foxtail millet.
276 We compared the divergence between the flanking tails in the LTRs (Suppl. Fig. 2) and
277 identified a single very recent burst of LTR *Gypsy* activity around 0.6 MYA (Kimura =
278 0.042 ± 0.026) and of LTR *Copia* also around 0.6 MYA (Kimura = 0.041 ± 0.027). Other
279 repeat elements, including LINEs (Long Interspersed Nuclear Elements), simple repeat

bioRxiv preprint doi: https://doi.org/10.1101/843870; this version posted November 17, 2019. The copyright holder for this preprint (which was not certified by peer review) is the author/funder, who has granted bioRxiv a license to display the preprint in perpetuity. It is made available under aCC-BY-ND 4.0 International license.

patterns of the sequence, satellites, and transposons were much less common, except for En/Spm DNA transposons observed in 4.2 % of the genome.

We annotated 42,232 coding genes, which included 42,359 predictive open reading frames (ORFs), as well as 875 non-coding genes without a predicted ORF (Suppl. file 2). Together these transcripts and non-coding genes define 43,234 targets for the expression analysis. 35,982 of the coding transcripts had a homologous protein in the NCBI non-redundant (*nr*) database. In 58% of the cases, the top hit was a *S. italica* sequence (Suppl. Fig. 3). Among those 35,982, 33,963 were functionally annotated with at least one GO term, and 39,488 had an InterPro annotation. We also identified the best reciprocal hit with *A. thaliana*, rice, *P. halli*, *S. italica* and *S. viridis*; and the top homologous in Uniprot (Suppl. File 3).

Comparative genomics with related grasses

Firstly, we aligned the transcripts and proteins from five sequenced species in the same clade, *S. italica*, *S. viridis* (L.) Beauv. (green foxtail), *Zea mays* L. (maize), *Panicum halli* Vasey and *P. virgatum* L. (switchgrass); and found that on average 78 % and 72 % of the transcripts and proteins aligned with an identity over 0.7, respectively (Suppl. Table 4).

We could assign 35,831 *Brachiaria* proteins to an eggNOG orthologous group (Powell et al. 2014), and 13,570 proteins could be further annotated with GO terms from the eggNOG database. We also assigned the proteins from other species in the Poaceae family to these eggNOG orthologous groups in order to identify shared clusters of proteins among these species. 24,752 of the total 26,354 clusters of proteins defined for Poaceae (poaVIR) in the eggNOG database could be found in at least one of the studied species, around 70 % common to the tribe Paniceae that includes *Setaria* and *Panicum* species, and around 60 % to all these five species in the subfamily Panicoideae (Suppl. File 4; Suppl. Fig. 4). More than 70% of the clusters of proteins had double or triple the number of proteins than other species because of relatively recent whole-genome duplication events. Around 85 % of the cluster in *S. italica*, *S. viridis* or *P. halli* contained only one protein from these species (Suppl. Table 5). The proportion is lower in *B. ruziziensis* and *Z. mays* and 20 % of the clusters had two proteins in both species. From this analysis, we also estimated that there are approximately two thousand proteins in other close species that are missed in our *Brachiaria* assembly.

bioRxiv preprint doi: https://doi.org/10.1101/843870; this version posted November 17, 2019. The copyright holder for this preprint (which was not certified by peer review) is the author/funder, who has granted bioRxiv a license to display the preprint in perpetuity. It is made available under aCC-BY-ND 4.0 International license.

We estimated the divergence between these species based on the Kimura divergence values between orthologous proteins in 6,450 clusters of proteins with one member from each species (*P. virgatum* was excluded from this analysis). The average Kimura divergence value for pairs of coding sequences of *B. ruziziensis* with *S. italica* was 0.094 ± 0.007, with *Panicum hallii* was 0.102 ± 0.007, with *S. viridis* was 0.095 ± 0.006, and with maize was 0.163 ± 0.008 (Suppl. Fig. 5). By assuming an average substitution rate of two-times (diploid) 1.3×10^{-8} (Schmutz et al. 2014), we estimated that *Brachiaria* diverged from the other Paniceae, *Setaria* and *Panicum*, around 13.4-15.5 million years ago (MYA), while the split of the Paniceae clades took place around 23.8-26.3 MYA (Suppl. Fig. 6).

The 23,076 scaffolds in the WGS longer than 10 Kbp or with at least one annotated gene (533.9 Mbp) were aligned in *S. italica* nine chromosomes, the closest relative with a high quality sequenced genome (Zhang et al. 2012). Up to 21,145 of the 23,076 scaffolds (91.6 %), which comprise 525.1 Mbp could be aligned (Fig 3; Suppl. file 5). Furthermore, this allowed us to assign chromosomal positions to 41,830 coding genes (41,974 transcripts) contained in these anchored sequences (Suppl. File 6). We identified 59 synteny blocks, 36 of which were longer than 1 Mbp in both species (Fig 3). There were three large translocations when comparing the *S. italica* and *B. ruziziensis* genomes between chromosomes 1 and 7, 2 and 6, as well as 3 and 5. And four inversions (smaller than the translocations) between tails in chromosomes 1 and 4 (both ends), 2 and 9 (proximal end), and 2 and 3 (proximal end).

QTL mapping in the interspecific *B. ruziziensis* X *B. decumbens* population

Between 78.8 and 91.5 % of the Genotyping-by-sequencing (GBS) reads from the 169 interspecific progeny and the progenitors' samples could be aligned in the assembly. After filtering, there was an average of 81,831 SNPs and 15,595 indels sites per sample. In total, 799,155 sites were called in the population. These sites were 85.7 % SNPs, 6.3 % insertions, 7.2 % deletions, 0.3 % mixed (a combination of SNPs and indels), and 0.5 % complex (expanding more than one bp). In agreement with filtering criteria previously tested in tetraploid *Brachiaria* samples (Worthington et al. 2016), we used SNPs only, and required at least 12 reads to call a homozygous site in any sample, a minimum allele frequency of 5 % and calls missing in less than 20 % of the samples. After filtering, 15,074 SNP sites were homozygous in the *B. ruziziensis* progenitor and heterozygous in the *B. decumbens* progenitor (nnxnp; Joinmap segregation descriptor, see Methods), 4,891 sites heterozygous in the *B. ruziziensis* progenitor and homozygous in the *B. decumbens* progenitor (lmxll), and

bioRxiv preprint doi: https://doi.org/10.1101/843870; this version posted November 17, 2019. The copyright holder for this preprint (which was not certified by peer review) is the author/funder, who has granted bioRxiv a license to display the preprint in perpetuity. It is made available under aCC-BY-ND 4.0 International license.

1,652 were heterozygous in both progenitors (hkxhk). We classified 4,817 nnxnp and 1,252 lmxll sites as single dose alleles (SDAs, or "simplex") based on their heterozygous/homozygous segregation ratio and used them as markers in the genetic map construction. The final genetic map included 4,427 markers placed at LOD 10 in 18 linkage groups (Suppl. Fig. 7, Suppl. File 7), which corresponds with the number of chromosomes expected in a tetraploid *Brachiaria* population such as this one. Linkage groups had an average length of 74.7 ± 22.7 cM. Based on the position of each SNP site in the genome, two linkage groups, relating to two homoelogous chromosomes, matched to each assembled chromosome (pseudomolecule), which were numbered following the order in *S. italica* (Suppl. Table 6). We also aligned the scaffolds in the genetic map to compare the co-linearity between the position of each marker in the genetic map and genome assembly (Suppl. Fig. 8).

As stated above, RL, RB and RD were scored in the interspecific population in control and Al^{3+} stress conditions. We also calculated the ratio between both conditions. 371 markers had marker/trait association LODs over 3, 273 markers in LG1, 73 markers in LG4, 51 markers in LG3, and 12, two and one in LGs 13, 10 and 5. 212 WGS scaffolds contained at least one marker with LOD over 3 (Suppl. File 7).

To identify well supported QTL, we focused on peaks with several consecutive significant markers based on a rolling average (window 3) LOD score over 4 (Fig. 4; Suppl. Fig. 9). This identified three QTLs each in LG 1 (Chr 8) for root length and biomass, LG 3 (Chr 7) for root length, and LG 4 (Chr 3) for root diameter. QTLs explained from 12.8 % to 16.1% of the phenotypic variance (Suppl. File 7). In a previous publication (Worthington et al. 2016), this population was phenotyped for reproductive mode (apomictic or sexual) using differential interference contrast (DIC) microscopy and the QTL mapped into Chromosome 1. Indeed, the apomictic locus (APO) was found again in LG7 (Chr 1), as previously reported (Worthington et al. 2019).

The peaks with the highest LOD values were observed in LG1 (Chr 8). A closer look evidenced several consecutive peaks in this QTL supported by both root length and biomass phenotypes. QTLs in the proximal region of the chromosome peaked at 7 cM (LOD 4.73) and 14.3 cM (LOD 4.95). An additional larger QTL is specific to control conditions peaked three times around 20.2-23.4, 25.7-26.2 and 27.6-28.8 cM, with the highest values at 26 cM for root length (LOD 5.8) and at 25.8 cM for root biomass (LOD 5.25). The QTL on LG 4 (Chr 3) peaked around 57.4-59 cM (LOD 4.3). The QTL in LG3 (Chr 7) showed two peaks at 96.8 cM for root length (LOD 4.75) and 79.7 cM for root diameter (LOD 4.02).

bioRxiv preprint doi: https://doi.org/10.1101/843870; this version posted November 17, 2019. The copyright holder for this preprint (which was not certified by peer review) is the author/funder, who has granted bioRxiv a license to display the preprint in perpetuity. It is made available under aCC-BY-ND 4.0 International license.

QTL regions contained 839 differentially expressed (DE) genes, of which 87 were differentially expressed (DE) (Suppl. file 8). Among the 87 differentially expressed genes in the QTL regions, 39 were in QTL in LG1, 17 were in the QTL in LG3, and 31 were in QTL in LG4. A total of 35 of the 87 genes were annotated as components of membrane, 18 were annotated as involved in response regulation, and 37 as binding to different molecular compounds, including ATP/ADP/GTP (12) and metal ions (9) and DNA (8). Only 12 of the 87 genes were not annotated with at least one of these previous GO terms. However, 17 of the 87 genes were uncharacterised proteins and not annotated with GO terms. All but six of these 17 had homologous proteins in the related grass species. All three QTL regions contained genes annotated in all the previous GO terms in approximately equal proportions.

Transcriptional differences during stress between *Brachiaria* species

We performed RNA-seq from stem and root tissue samples extracted from the *B. decumbens* and *B. ruziziensis* progenitors after growing for three days in control or high (200 µM $AlCl^3$) aluminium cation concentration hydroponic solutions. We also incorporated a reference-based reanalysis of public RNA-seq data (PRJNA314352) of the aluminium-resistant *B. decumbens* var. Basilisks roots (referred to as “Basilisks” in this paper, while *B. decumbens* always refers to cultivar CIAT 606) screened using the same experimental conditions and treatments as employed by us (Salgado et al. 2017).

When the normalised counts for all the genes were used to cluster the samples, these clusters firstly grouped by tissue, secondly by genotype, and thirdly by treatment (Suppl. Fig. 10). As a consequence, the following results comparing control against stress treatment are presented according to species and tissue. There were 5,421 DE genes in total, with most of these differentially regulated in a single genotype and tissue (Suppl. Fig. 11). Among these, 5102 were DE in roots only, 249 in stems only, and 70 in both tissues. Up to 116 of the DE genes were non-coding (without a clear ORF).

4,423 of the 5,102 genes DE in roots were specific to one of the species (Fig. 5). We obtained twice as many DE genes in *B. ruziziensis* as in the other two species. The proportion of DE genes specific to only one species was maintained when considering up- and down-regulated genes separately. The most substantial overlaps between gene sets were between *B. ruziziensis* and *B. decumbens*, with 178 genes up-regulated and 154 gene down-regulated in both. f86 genes were up-regulated genes in both *B. decumbens* cv. CIAT

bioRxiv preprint doi: https://doi.org/10.1101/843870; this version posted November 17, 2019. The copyright holder for this preprint (which was not certified by peer review) is the author/funder, who has granted bioRxiv a license to display the preprint in perpetuity. It is made available under aCC-BY-ND 4.0 International license.

606 and cv. Basilisks, and 67 genes were up-regulated in Basilisks but down-regulated in *B. ruziziensis*.

Enrichment analysis of the GO terms over-represented among DE genes in each species allowed us to identify the biological processes (BP) and molecular functions (MF) that are similarly or differently regulated among them (Suppl. File 9 and 10). After annotating the genes with the full set of GO terms as described previously, we simplified the results to "GO slim" terms for this analysis. "GO slim" contains the subset of higher-level terms from the GO resource (Fig. 6, sorted left to right from high to low tolerance to Al^{3+} toxic levels; Statistical analysis in Suppl. Table 7).

There was little overlap among GO terms based on the DE genes included in each annotation, as represented in a correlation matrix plot (Suppl. Fig. 12). The exception is the overlap between five MF terms related to RNA/mRNA/rRNA binding with the ribosome (MF:3723, 3729, 19843; and 3735 and 5198) among themselves and with two BP terms, namely "translation" and "ribonucleoprotein complex assembly" (BP: 6412, 22618). All these terms were significantly enriched among down-regulated genes in *B. ruziziensis* and *B. decumbens*, but were not enriched in Basilisks. The number of genes was much larger in *B. ruziziensis* (146 genes) than *B. decumbens* or Basilisks (39 and 16 genes, respectively). Most of these genes were annotated as ribosomal RPS/RPL proteins.

Despite little overlap among gene sets, the number of enriched GO terms was similar between different species. The exception to this observation wass "ion binding" and the translation-related GO terms in *B. ruziziensis*.

Genes annotated as "transmembrane transporters" (MF:22857) were highly over-represented (Fisher's test values in Suppl. Table 7) among up-regulated DE genes in all three species (57 in Basilisks, 44 in *B. decumbens* and 70 in *B. ruziziensis*). This annotation was also highly represented among down-regulated DE genes in Basilisks (16 genes). However, only two were common to the three species, a MST3 sugar transporter (Gene 1766G4) and 8448G4, a STAR1/ALS1 aluminium-induced transmembrane ABC transporter (Huang et al. 2009). While most of these genes were DE in only one of the species (only 21 were shared between any two species), they appear to cover similar roles in all three species as "ABC transporters", "P-type ATPases" and "Amino acid transporters". As commented before, there was a minimal overlap between this GO term (MF:22857) and the "transmembrane transport" BP term (BP:55085), which was only enriched in Basilisks and includes a small number of proteins (seven in Basilisk and *B. ruziziensis*, and three in *B.*

bioRxiv preprint doi: https://doi.org/10.1101/843870; this version posted November 17, 2019. The copyright holder for this preprint (which was not certified by peer review) is the author/funder, who has granted bioRxiv a license to display the preprint in perpetuity. It is made available under aCC-BY-ND 4.0 International license.

decumbens). Most of these proteins were annotated as mitochondrial transporters, but three of the 7 Basilisks-specific DE genes were annotated as tonoplast and vacuolar transporters induced by abiotic stress and involved in functions "critical for pH homeostasis" (Genes 211G30, 211G34 and 751G28).

Four functions were regulated in *B. ruziziensis* differently than in the other species (Fig. 6), "cell wall organization and biogenesis" (BP:71554), transport (BP:6810), ion binding (MF:43167) and glycosyl hydrolase activity (MF:16757). The "biosynthetic process" term (BP:9058) was enriched in both down-regulated and up-regulated DE genes in *B. ruziziensis* (Suppl. Fig. 13).

"Cell wall organization and biogenesis" included 51 down-regulated DE genes in *B. ruziziensis*, while included only 14/17 up-regulated DE genes in the other species. Most of these in either species were peroxidases PER and expansin proteins induced by various plant hormones (ethylene, GA, auxin, etc.) and involved in toxic removal during oxidative stress (Kochian et al. 2015).

"Transport" was enriched among up-regulated genes in *B. decumbens* and down-regulated genes in *B. ruziziensis*, and not enriched in Basilisks. It included 83, 35 and 12 DE genes in *B. ruziziensis*, *B. decumbens* and Basilisks, respectively. In all species, these proteins were localizing different substances (phosphate, sodium, mRNA, etc.) to various cell organelles. Only two genes were common to *B. ruziziensis* and *B. decumbens* and so regulated in opposite ways: a manganese metal-binding intracellular transporter involved in root development (7811G2) and a GTP-binding protein involved in nucleocytoplasmic transport (14972G2). Up-regulated genes in *B. decumbens* were also up-regulated in *B. ruziziensis*, but with lower values of fold-change expressions. Exceptionally, six of the 35 exhibited high fold-changes in both species. These highlighted DE genes were involved in phospholipids, phosphate, magnesium, auxin, nitrate and miRNA transport in the cell (Genes 6944G2, 12087G2, 8068G4, 26018G2, 4534G2, 2708G4).

"Ion binding" was only enriched in *B. ruziziensis* (100 up-regulated genes), though 44 and 26 DE genes in *B. decumbens* and Basilisks, respectively, were also up-regulated in those species. Ten genes were DE in both *B. decumbens* and *B. ruziziensis* with functions, such as "nitrate assimilation" (26018G2 -again- and 122G16), "phospholipid translocation" (6944G2 again), and "phytic acid -phosphorus storage- trafficking" (87018G2 and 89122G2).

bioRxiv preprint doi: https://doi.org/10.1101/843870; this version posted November 17, 2019. The copyright holder for this preprint (which was not certified by peer review) is the author/funder, who has granted bioRxiv a license to display the preprint in perpetuity. It is made available under aCC-BY-ND 4.0 International license.

"Glycosyl hydrolase" was enriched among down-regulated genes in *B. ruziziensis* (39 genes), but among up-regulated genes in both *B. decumbens* and Basilisks (18 and 24 genes, respectively). Again, there was little overlap among these gene sets. In *B. ruziziensis*, ten of the 39 down-regulated genes were associated with different "defense response". The same proportion was observed among up-regulated *B. decumbens* and Basilisks genes. There was overlap between "Glycosyl hydrolase" and "carbohydrate metabolism" (BP:5975) (Suppl Fig. 13), which, in principle, shows the same enrichment pattern, down-regulated in *B. ruziziensis* (42 genes) but up-regulated in the other species (24 and 21 genes in Basilisks and *B. decumbens*, respectively). However, "carbohydrate metabolism" (BP:5975) was also enriched among down-regulated DE genes in Basilisks (13 genes). Similar specific GO terms and pathways were enriched in either up- or down-regulated genes, such as "hemicellulose metabolic process", xyloglucan metabolism, glycoside hydrolases, "sucrose degradation" pathways.

Two GO terms, "oxidoreductase activity" (MF:16491) and "small molecule metabolism" (BP:44281) were enriched in both up-regulated and down-regulated genes in Basilisks (69 and 29 genes, respectively), but, in both cases, were only enriched among down-regulated genes in *B. ruziziensis* and *B. decumbens* (Suppl. Fig. 13). There were fewer up-regulated genes in these species than in Basilisks.

DISCUSSION

Forward genetics and newly produced genomic resources to identify candidate loci for abiotic stress tolerance

The negative effects of soil acidity on crop production are essentially associated with different mineral toxicities and deficiencies. Aluminium cation toxicity has long been established to be the single most important limiting factor associated with acidic soil productivity (Eswaran, Reich, and Beinroth 1997).

All *Brachiaria* species show some tolerance to Al^{3+} toxicity, particularly compared with other grasses such as wheat, rice and maize (Kochian et al. 2015; Arroyave et al. 2013). While most crops reduce root growth to 50 % when exposed to 5 µM Al^{3+}, *Brachiaria* species need to be exposed to up to 35 µM to exhibit a reduced root growth of 25 % (Poschenrieder et al. 2008).

bioRxiv preprint doi: https://doi.org/10.1101/843870; this version posted November 17, 2019. The copyright holder for this preprint (which was not certified by peer review) is the author/funder, who has granted bioRxiv a license to display the preprint in perpetuity. It is made available under aCC-BY-ND 4.0 International license.

Natural plant adaptation to acid soils can be measured by estimating root vigour in low pH soils and resistance to high concentrations of Al^{3+} (Wenzl et al. 2006). In our experiment, *B. decumbens*-CIAT606 root morphology was less affected than *B. ruziziensis*-BRX4404 after growing for 3 and 20 days in control and high 200 µM Al^{3+} concentration hydroponic solutions, for tissue sampling (RNA-seq analysis) and phenotyping (QTL analysis), respectively. In our differential expression analysis, we have compared low tolerant or sensitive (*B. ruziziensis* BRX 44-02), intermediate (*B. decumbens* cv. CIAT 606) and high tolerant or resistant (*B. decumbens* cv. Basilisks) accessions by including in the work a reanalysis of the *B. decumbens* basilisk RNA-seq data from Salgado *et al.* (2017), which was produced under the same experimental conditions as ours but did not use a reference genome. As a comparison, in a 21-day long term study using a similar screening, four *B. decumbens* and four *B. ruziziensis* genotypes showed intermediate tolerance of Al^{3+}, one *B. ruzizensis* genotype was sensitive, and only the *B. decumbens* cultivar Basilisk was unaffected by high Al^{3+} (Bitencourt et al. 2011). Interestingly, Furlan *et al.* (2018) recently reported a higher Al^{3+} tolerance in *B. brizantha* cv. Xaraes than in *B. decumbens* cv. Basilisks.

We contrasted *B. ruziziensis* and *B. decumbens* hybrid progeny to understand their differences in tolerance further. We measured adaptive roots traits to soils with toxic concentrations of aluminium and identified QTLs for all the root traits scored and segregating in the interspecific population. The three QTLs we identified were not large effect (LOD scores under 6) but were observed for several root traits. Also, they may not have been directly related to aluminium resistant but more to general root vigour. In future work, it will be interesting to see if these QTLs are also associated with drought tolerance, since this trait is also affected by root architecture (Uga et al. 2013). Our results integrating QTLs and differential expression analysis highlighted the importance of membrane transport (including metal ions), regulation and signalling (binding to DNA), and energy (carbohydrate metabolism and binding to ATP/ADP/GTP) molecular mechanisms. The most aluminium-tolerant *Brachiaria*, cultivar Xaraes, accumulated the largest concentration of aluminium in roots. How *B. decumbens* avoids the apoplastic binding of Al^{3+}, as other resistant crops do, remains unknown. However, both tolerant cultivars, Xaraes and Basilisk, kept oxidative stress lower than other genotypes under increasing Al^{3+} concentrations (Furlan et al. 2018).

We are also making publicly available the genome assembly and gene annotation of a diploid *Brachiaria ruziziensis*. This genome provides a necessary platform for genomic approaches for trait improvement. Our transcriptomic study and comparative genomics

bioRxiv preprint doi: https://doi.org/10.1101/843870; this version posted November 17, 2019. The copyright holder for this preprint (which was not certified by peer review) is the author/funder, who has granted bioRxiv a license to display the preprint in perpetuity. It is made available under aCC-BY-ND 4.0 International license.

573 analysis are examples of its utility. We opted for a non-polyploid diploid accession because
574 *Brachiaria* grasses are heterozygous outcrossing species. While tetraploid *B. ruziziensis* are
575 the main accessions used for breeding new hybrids, artificially induced doubled diploids
576 allow the generation of hybrid sexual progeny which increases the available genetic
577 diversity (Worthington and Miles 2015; Simioni and do Valle 2009). This genome is the
578 diploid accession that was chromosome-doubled with colchicine to produce the
579 autotetraploid *B. ruziziensis* progenitor of the interspecific population analysed.
580
581 The assembly was partially scaffolded to pseudomolecule level using a genetic map which
582 contained approximately 5,000 markers. This genetic map had previously been assembled
583 without a reference genome (Worthington et al. 2016), but a higher number of markers could
584 be sorted using this new reference. Long reads will improve this assembly and allow for
585 polyploid genome references in the near future. Because of the limited number of markers,
586 almost all the scaffolds were also placed on the high-quality *S. italica* genome. While we
587 identified three large chromosomal transpositions (Chromosomes 5, 6 and 7), gene order on
588 all pairs of chromosomes was highly conserved between the two species as previously
589 observed (Worthington et al. 2016) and as might be predicted from species diverging only
590 13-15 MYA.
591
592
593 **Differentially expressed genes associated with tolerance to Al^{3+} in *Brachiaria***
594
595 Aluminium tolerance mechanisms are classified as external exclusion or internal tolerance
596 mechanisms (Kochian et al. 2015; Furlan et al. 2018). Internal tolerance mechanisms
597 involve either modification of the properties of the root cell wall, or the uptake and
598 sequestration of Al^{3+} once it enters the plant (Kochian et al. 2015). Ramos *et al.* (2012)
599 observed that *B. decumbens* accumulated Al^{3+} in the mucilage layer of root apices, which
600 reduced the quantity of Al^{3+} reaching the cell wall and crossing the plasma membrane.
601 Arroyave *et al.* (2013) suggested that the presence of a complex exodermis in *B.*
602 *decumbens*, that is absent in *B. ruziziensis*, may contribute to a more efficient exclusion of
603 Al^{3+}. On the other hand, a higher concentration of root pectin measured in *B. ruziziensis*
604 during stress can evidence increased apoplastic aluminium binding (Horst, Wang, and
605 Eticha 2010). Changes in the structural properties of cell wall carbohydrates are mediated by
606 expansins, endo-β-1,4-glucanases, xyloglucan transferases and hydrolases (XTH) (e.g.
607 AtXTH31 and AtXTH15) and pectin methylesterases (Yang et al. 2011; Kochian et al. 2015).
608 Contrasting regulation, as evidenced by differences in enriched GO terms between *B.*
609 *decumbens* and *B. ruziziensis* suggest *B. decumbens* adaptations may be associated with

bioRxiv preprint doi: https://doi.org/10.1101/843870; this version posted November 17, 2019. The copyright holder for this preprint (which was not certified by peer review) is the author/funder, who has granted bioRxiv a license to display the preprint in perpetuity. It is made available under aCC-BY-ND 4.0 International license.

xyloglucan transferring (GO:16762) and oxidation (GO:52716). This contrasting enrichment was largely due to 12 differentially expressed XTH proteins that are down-regulated during stress in *B. ruziziensis*, but not in *B. decumbens*. One of them (5400G2) is in the QTL region in LG1. There are three additional differentially expressed XTH proteins that are up-regulated: 5233G2 (AtXTH23) only in *B. decumbens*, and 6544G2 (AtXTH32) and 11683G4 (AtXTH27), which are up-regulated in both *B. decumbens* and *B. ruziziensis*. Among the 20 non-DE XTH proteins in the genome, these showed the highest homology to XTH31 (554G10, 99G28) and XTH15 (385G24). The *Brachiaria* gene with closest homology to SLK2 (1984G2) is upregulated in both *B. ruziziensis* and *B. decumbens*, but only DE in *B. decumbens*. AtSLK2 is involved in cell wall pectin methylesterification in response to Al^{3+} stress (Geng et al. 2017). The "glycosyl hydrolase" GO term was enriched by down-regulated genes in *B. ruziziensis* (39 genes), but by up-regulated genes in both *B. decumbens* and Basilisks (18 and 24 genes, respectively).

Once Al^{3+} has entered the root, the uptake and sequestration of Al^{3+} includes molecular binding and eventually compartmentation of the toxic substance. ALS (Aluminium Sensitive) transporters and NRAM metal ion transporters have been proposed as keystones in Al^{3+} localization to the tonoplast and other cell organelles, and away from the sensitive root tips in *A. thaliana* and rice (Larsen et al. 2007; Huang, Yamaji, and Ma 2010; Huang et al. 2012). Notably, an NRAM aluminium transporter (NRAT1) localized in the plasma membrane appears to be expressly involved in storing Al^{3+} in root vacuoles in rice and maize (Xia et al. 2010; Guimaraes et al. 2014). In *Brachiaria*, we identified 21 NRAM proteins. However, only three of them were DE: a gene that with homology to OsTITANIA (AtOBE3/ATT1), which is transcription factor (2499G8) that functions as a regulator of NRAM and other metal transporter genes (Tanaka et al. 2018) and two of the three *Brachiaria* proteins showing close homology to OsNRAT1, 3672G6 and 30107G2. These were, significantly up-regulated in both *B. decumbens* and *B. ruziziensis* during stress. The third gene, with close homology to OsNRAT1, was not DE (1881G2). Eight genes in the *Brachiaria* genome are homologous to ALS1 and annotated as aluminum-induced ABC transporters, but only gene 3096G6 was DE in *B. ruziziensis*. However, it was not-significantly up-regulated in *B. decumbens*.

In rice, the complex formed by STAR1 and STAR2/AtALS3 (Sensitive To Aluminium Rhizotoxicity) is involved in aluminium-induced alterations of the cell wall composition related to less aluminium-binding in the apoplast (Huang, Yamaji, and Ma 2010; Huang et al. 2009). These ABC transporters appear to mediate the efflux of UDP-glucose into the cell wall, which could alter the cell wall composition and lead to a reduction in Al-binding capacity (Kochian et al. 2015). Fifteen proteins had homology to STAR/ALS in *Brachiaria*, but only

bioRxiv preprint doi: https://doi.org/10.1101/843870; this version posted November 17, 2019. The copyright holder for this preprint (which was not certified by peer review) is the author/funder, who has granted bioRxiv a license to display the preprint in perpetuity. It is made available under aCC-BY-ND 4.0 International license.

two were DE: gene 8448G4 had closest homology with OsSTAR1 and gene 7361G2 with OsSTAR2 and AtALS3. STAR1/STAR2 were up-regulated in both *B. ruziziensis* and *B. decumbens*. Over 150 genes annotated with the "transmembrane transporters" GO term (MF:22857) were highly overrepresented among up-regulated DE genes in all three species (57 in Basilisks, 44 in *B. decumbens* and 70 in *B. ruziziensis*), and two were common to the three species: a MST3 sugar transporter (Gene 1766G4) and the previously highlighted STAR1/ALS1 (8448G4) .

Most aluminium tolerant crops additionally rely on external restriction to prevent the uptake of aluminium and its entry into the root cells through the release of anionic organic acids in the rhizosphere that chelate the Al^{3+} (Rao et al. 2016; Kochian et al. 2015). However, *Brachiaria* appears to not rely on secreted organic acids since no clear relation between aluminium-induced organic acid efflux from roots and resistance could be established, there was no difference in secreted organic acids between tolerant and resistant *Brachiaria* species (Wenzl et al. 2001; Arroyave et al. 2013). Furthermore, tolerant *B. decumbens* accessions secreted 3-30 times less organic acids than sensitive species such as maize and wheat (Wenzl et al. 2001; Arroyave et al. 2018). However, while *B. decumbens* citrate exudation was about 200 times lower than that observed in aluminium-tolerant rice, the same study evidenced high oxalate exudation in *B. decumbens* roots, but only between 24 and 36 hours after exposure to the toxic concentration (Arroyave et al. 2018). It appears that other mechanisms of resistance overshadow the impact of root exudation. The lack of correlation between exudation and resistance has also been observed in rice (Famoso et al. 2010; Ma et al. 2002).

Two families of membrane transporters, aluminium-activated malate transporter (ALMT) and the multidrug and toxic compound extrusion (MATE) family, are responsible for plasma membrane malate and citrate efflux, respectively (Raman et al. 2005; Guimaraes et al. 2014; Rao et al. 2016). Citrate is a much stronger chelating agent for Al^{3+} than malate (Ma 2000). In rice, FRDL4 is responsible for aluminium-induced citrate efflux required for external detoxification (Yokosho, Yamaji, and Ma 2011). In *Brachiaria*, we identified three citrate transporters MATE proteins, which could be characterised as FRDL (Ferric Reductase Defective Like) proteins, 61G2 in *B. decumbens*, and 259G14 and 675G12 in both *B. decumbens* and *B. ruziziensis*. All 3 were differentially upregulated with large fold-changes, particularly 675G12.

Given their role in Al^{3+} tolerance in other grasses, we identified thirteen aluminium-activated malate transporters (AMLTs) in the genome. However, only two were differentially

bioRxiv preprint doi: https://doi.org/10.1101/843870; this version posted November 17, 2019. The copyright holder for this preprint (which was not certified by peer review) is the author/funder, who has granted bioRxiv a license to display the preprint in perpetuity. It is made available under aCC-BY-ND 4.0 International license.

684 expressed: 11634G4 was up-regulated 4.74 fold-change during stress in *B. decumbens*, and
685 462G24 was down-regulated 2.35 fold-change in *B. ruziziensis*. We identified a cluster with
686 three contiguous non-DE AMLTs (5136G2, 5136G4 and 5136G6) in scaffold 5136 (LG3:
687 71.83-72.95 cM) around 10 cM from the QTL. This is consistent with the observation that
688 copy-number variation of ALMT correlated with aluminium resistance in rye and maize
689 (Collins et al. 2008; Maron et al. 2013). However, a more precise understanding of the
690 discrepancies between the early 24-to-36 hours "alarm phase" and the long-term resistance
691 mechanisms would be necessary to understand the role of aluminium-activated malate
692 transporters and citrate efflux in *Brachiaria*.
693
694 C_2H_2-type zinc-finger transcription factors STOP1 (ART1 in rice) and STOP2 regulate
695 aluminium-induced expression of several MATE and ALMT genes in Arabidopsis and rice
696 (Iuchi et al. 2007; Yamaji et al. 2009; Kobayashi et al. 2014). We identified three genes with
697 homology to AtSTOP1, one was DE in *B. ruziziensis* (29G2) and another two (3833G12 and
698 243G34) which were not DE. We also identified two genes with homology to AtSTOP2, both
699 were upregulated with high fold-change in *B. ruziziensis* and *B. decumbens* (126G26 and
700 1615G2). All five had homology with OsART1, the STOP1 homolog in rice, which up-
701 regulated at least 31 genes in an Al-dependent manner, including STAR1, FRDL, NRAMP
702 proteins (Yamaji et al. 2009; Kochian et al. 2015).
703
704
705 **CONCLUSION**
706
707 In this work we present a comprehensive analysis of the molecular mechanism linked to
708 aluminium tolerance in *Brachiaria* species. Phenotypic studies on root development allowed
709 us to identify genotypes that present tolerance to aluminium. By sequencing, assembly and
710 annotating a diploid genotype of *Brachiaria ruzinzensis* we have developed the capability for
711 genomic-based studies of desirable phenotypic traits. Using this resource, we have identified
712 three QTLs associated to root vigour that where followed up/complemented by
713 transcriptomic profiling of a range of 3 contrasting genotypes subject to aluminium stress
714 treatments. We have identified a number of genes and molecular responses that impact on
715 different aspects of signalling, cell-wall composition and active transports as response to
716 aluminium stress. We found that external mechanisms such sequestration of Al^{3+} common in
717 other grasses might be not that important in *Brachiaria* and that among different Brachiaria
718 species the timing and intensity of the response can explain the different levels of tolerance.
719 Finally, the newly annotated draft genome represents an important base upon which study
720 other aspects of *Brachiaria* biology.

bioRxiv preprint doi: https://doi.org/10.1101/843870; this version posted November 17, 2019. The copyright holder for this preprint (which was not certified by peer review) is the author/funder, who has granted bioRxiv a license to display the preprint in perpetuity. It is made available under aCC-BY-ND 4.0 International license.

REFERENCES

Alexa, Adrian, and Jorg Rahnenfuhrer. 2010. 'topGO: enrichment analysis for gene ontology', *R package version*, 2: 2010.

Andrews, Simon. 2017. "FastQC: a quality control tool for high throughput sequence data. 2010." In.

Arroyave, Catalina, Juan Barceló, Charlotte Poschenrieder, and Roser Tolrà. 2011. 'Aluminium-induced changes in root epidermal cell patterning, a distinctive feature of hyperresistance to Al in Brachiaria decumbens', *Journal of inorganic biochemistry*, 105: 1477-83.

Arroyave, Catalina, Roser Tolrà, Livia Chaves, Marcelo Claro de Souza, Juan Barceló, and Charlotte Poschenrieder. 2018. 'A proteomic approach to the mechanisms underlying activation of aluminium resistance in roots of Urochloa decumbens', *Journal of inorganic biochemistry*, 181: 145-51.

Arroyave, Catalina, Roser Tolrà, Thanh Thuy, Juan Barceló, and Charlotte Poschenrieder. 2013. 'Differential aluminum resistance in Brachiaria species', *Environmental and experimental botany*, 89: 11-18.

Bailey-Serres, Julia, Jane E Parker, Elizabeth A Ainsworth, Giles ED Oldroyd, and Julian I Schroeder. 2019. 'Genetic strategies for improving crop yields', *Nature*, 575: 109-18.

Bitencourt, Gislayne de Araujo, Lucimara Chiari, Valdemir Antônio Laura, Cacilda Borges do Valle, Liana Jank, and José Roberto Moro. 2011. 'Aluminum tolerance on genotypes of signal grass', *Revista Brasileira de Zootecnia*, 40: 245-50.

Cabanettes, Floréal, and Christophe Klopp. 2018. 'D-GENIES: dot plot large genomes in an interactive, efficient and simple way', *PeerJ*, 6: e4958.

Caniato, FF, CT Guimaraes, RE Schaffert, VMC Alves, LV Kochian, A Borém, PE Klein, and JV Magalhaes. 2007. 'Genetic diversity for aluminum tolerance in sorghum', *Theoretical and Applied Genetics*, 114: 863-76.

Collins, NC, NJ Shirley, Muhammad Saeed, Margaret Pallotta, and JP Gustafson. 2008. 'An ALMT1 gene cluster controlling aluminum tolerance at the Alt4 locus of rye (Secale cereale L.)', *Genetics*, 179: 669-82.

Conesa, Ana, Stefan Götz, Juan Miguel García-Gómez, Javier Terol, Manuel Talón, and Montserrat Robles. 2005. 'Blast2GO: a universal tool for annotation, visualization and analysis in functional genomics research', *Bioinformatics*, 21: 3674-76.

De Vega, Jose J, Sarah Ayling, Matthew Hegarty, Dave Kudrna, Jose L Goicoechea, Åshild Ergon, Odd A Rognli, Charlotte Jones, Martin Swain, and Rene Geurts. 2015. 'Red clover (Trifolium pratense L.) draft genome provides a platform for trait improvement', *Scientific reports*, 5: 17394.

bioRxiv preprint doi: https://doi.org/10.1101/843870; this version posted November 17, 2019. The copyright holder for this preprint (which was not certified by peer review) is the author/funder, who has granted bioRxiv a license to display the preprint in perpetuity. It is made available under aCC-BY-ND 4.0 International license.

758 Dobin, Alexander, Carrie A Davis, Felix Schlesinger, Jorg Drenkow, Chris Zaleski, Sonali
759 Jha, Philippe Batut, Mark Chaisson, and Thomas R Gingeras. 2013. 'STAR: ultrafast
760 universal RNA-seq aligner', *Bioinformatics*, 29: 15-21.
761 Edgar, Robert C. 2004. 'MUSCLE: multiple sequence alignment with high accuracy and high
762 throughput', *Nucleic acids research*, 32: 1792-97.
763 Ellinghaus, David, Stefan Kurtz, and Ute Willhoeft. 2008. 'LTRharvest, an efficient and
764 flexible software for de novo detection of LTR retrotransposons', *BMC bioinformatics*,
765 9: 18.
766 English, Adam C, Stephen Richards, Yi Han, Min Wang, Vanesa Vee, Jiaxin Qu, Xiang Qin,
767 Donna M Muzny, Jeffrey G Reid, and Kim C Worley. 2012. 'Mind the gap: upgrading
768 genomes with Pacific Biosciences RS long-read sequencing technology', *PloS one*,
769 7: e47768.
770 Eswaran, H, P Reich, and F Beinroth. 1997. 'Global distribution of soils with acidity', *Plant-*
771 *Soil interactions at low pH*: 159-64.
772 Famoso, Adam N, Randy T Clark, Jon E Shaff, Eric Craft, Susan R McCouch, and Leon V
773 Kochian. 2010. 'Development of a novel aluminum tolerance phenotyping platform
774 used for comparisons of cereal aluminum tolerance and investigations into rice
775 aluminum tolerance mechanisms', *Plant physiology*, 153: 1678-91.
776 Furlan, Felipe, Lucelia Borgo, Flávio Henrique Silveira Rabêlo, Monica Lanzoni Rossi,
777 Adriana Pinheiro Martinelli, Ricardo Antunes Azevedo, and José Lavres. 2018.
778 'Aluminum-induced stress differently modifies Urochloa genotypes responses on
779 growth and regrowth: root-to-shoot Al-translocation and oxidative stress', *Theoretical*
780 *and Experimental Plant Physiology*, 30: 141-52.
781 Geng, Xiaoyu, Walter J Horst, John F Golz, Joanne E Lee, Zhaojun Ding, and Zhong-Bao
782 Yang. 2017. 'LEUNIG _ HOMOLOG transcriptional co-repressor mediates aluminium
783 sensitivity through PECTIN METHYLESTERASE 46-modulated root cell wall pectin
784 methylesterification in Arabidopsis', *The Plant Journal*, 90: 491-504.
785 Grabherr, Manfred G, Brian J Haas, Moran Yassour, Joshua Z Levin, Dawn A Thompson,
786 Ido Amit, Xian Adiconis, Lin Fan, Raktima Raychowdhury, and Qiandong Zeng.
787 2011. 'Full-length transcriptome assembly from RNA-Seq data without a reference
788 genome', *Nature biotechnology*, 29: 644.
789 Guimaraes, Claudia T, Christiano C Simoes, Maria Marta Pastina, Lyza G Maron, Jurandir V
790 Magalhaes, Renato CC Vasconcellos, Lauro JM Guimaraes, Ubiraci GP Lana,
791 Carlos FS Tinoco, and Roberto W Noda. 2014. 'Genetic dissection of Al tolerance
792 QTLs in the maize genome by high density SNP scan', *BMC genomics*, 15: 153.
793 Hede, AR, B Skovmand, and J Lopez Cesati. 2001. "Acid soils and aluminum toxicity.
794 Application of Physiology in Wheat Breeding." In.

bioRxiv preprint doi: https://doi.org/10.1101/843870; this version posted November 17, 2019. The copyright holder for this preprint (which was not certified by peer review) is the author/funder, who has granted bioRxiv a license to display the preprint in perpetuity. It is made available under aCC-BY-ND 4.0 International license.

795 Horst, Walter J, Yunxia Wang, and Dejene Eticha. 2010. 'The role of the root apoplast in
796 aluminium-induced inhibition of root elongation and in aluminium resistance of plants:
797 a review', *Annals of Botany*, 106: 185-97.
798 Huang, Chao Feng, Naoki Yamaji, Namiki Mitani, Masahiro Yano, Yoshiaki Nagamura, and
799 Jian Feng Ma. 2009. 'A bacterial-type ABC transporter is involved in aluminum
800 tolerance in rice', *The Plant Cell*, 21: 655-67.
801 Huang, Chao-Feng, Naoki Yamaji, and Jian Feng Ma. 2010. 'Knockout of a bacterial-type
802 ATP-binding cassette transporter gene, AtSTAR1, results in increased aluminum
803 sensitivity in Arabidopsis', *Plant physiology*, 153: 1669-77.
804 Huang, Chao-Feng, Naoki Yamaji, Zhichang Chen, and Jian Feng Ma. 2012. 'A
805 tonoplast-localized half-size ABC transporter is required for internal detoxification of
806 aluminum in rice', *The Plant Journal*, 69: 857-67.
807 Huerta-Cepas, Jaime, Kristoffer Forslund, Luis Pedro Coelho, Damian Szklarczyk, Lars Juhl
808 Jensen, Christian von Mering, and Peer Bork. 2017. 'Fast genome-wide functional
809 annotation through orthology assignment by eggNOG-mapper', *Molecular biology
810 and evolution*, 34: 2115-22.
811 Iuchi, Satoshi, Hiroyuki Koyama, Atsuko Iuchi, Yasufumi Kobayashi, Sadako Kitabayashi,
812 Yuriko Kobayashi, Takashi Ikka, Takashi Hirayama, Kazuo Shinozaki, and
813 Masatomo Kobayashi. 2007. 'Zinc finger protein STOP1 is critical for proton
814 tolerance in Arabidopsis and coregulates a key gene in aluminum tolerance',
815 *Proceedings of the National Academy of Sciences*, 104: 9900-05.
816 Johnson, James P, Brett F Carver, and VC Baligar. 1997. 'Expression of aluminum tolerance
817 transferred from Atlas 66 to hard winter wheat', *Crop Science*, 37: 103-08.
818 Kajitani, Rei, Kouta Toshimoto, Hideki Noguchi, Atsushi Toyoda, Yoshitoshi Ogura, Miki
819 Okuno, Mitsuru Yabana, Masayuki Harada, Eiji Nagayasu, and Haruhiko Maruyama.
820 2014. 'Efficient de novo assembly of highly heterozygous genomes from whole-
821 genome shotgun short reads', *Genome research*, 24: 1384-95.
822 Kobayashi, Yuriko, Yoshinao Ohyama, Yasufumi Kobayashi, Hiroki Ito, Satoshi Iuchi, Miki
823 Fujita, Cheng-Ri Zhao, Tazib Tanveer, Markkandan Ganesan, and Masatomo
824 Kobayashi. 2014. 'STOP2 activates transcription of several genes for Al-and low pH-
825 tolerance that are regulated by STOP1 in Arabidopsis', *Molecular plant*, 7: 311-22.
826 Kochian, Leon V, Miguel A Piñeros, Jiping Liu, and Jurandir V Magalhaes. 2015. 'Plant
827 adaptation to acid soils: the molecular basis for crop aluminum resistance', *Annual
828 Review of Plant Biology*, 66: 571-98.
829 Larsen, Paul B, Jesse Cancel, Megan Rounds, and Vanessa Ochoa. 2007. 'Arabidopsis
830 ALS1 encodes a root tip and stele localized half type ABC transporter required for
831 root growth in an aluminum toxic environment', *Planta*, 225: 1447.

bioRxiv preprint doi: https://doi.org/10.1101/843870; this version posted November 17, 2019. The copyright holder for this preprint (which was not certified by peer review) is the author/funder, who has granted bioRxiv a license to display the preprint in perpetuity. It is made available under aCC-BY-ND 4.0 International license.

Leggett, Richard M, Bernardo J Clavijo, Leah Clissold, Matthew D Clark, and Mario Caccamo. 2013. 'NextClip: an analysis and read preparation tool for Nextera Long Mate Pair libraries', *Bioinformatics*, 30: 566-68.

Leggett, Richard Mark, Ricardo Humberto Ramirez-Gonzalez, Bernardo Clavijo, Darren Waite, and Robert Paul Davey. 2013. 'Sequencing quality assessment tools to enable data-driven informatics for high throughput genomics', *Frontiers in genetics*, 4: 288.

Li, Heng. 2013. 'Aligning sequence reads, clone sequences and assembly contigs with BWA-MEM', *arXiv preprint arXiv:1303.3997*.

———. 2016. 'Minimap and miniasm: fast mapping and de novo assembly for noisy long sequences', *Bioinformatics*, 32: 2103-10.

Love, Michael I, Wolfgang Huber, and Simon Anders. 2014. 'Moderated estimation of fold change and dispersion for RNA-seq data with DESeq2', *Genome biology*, 15: 550.

Ma, Jian Feng. 2000. "Role of organic acids in detoxification of aluminum in higher plants." In.

Ma, Jian Feng, Renfang Shen, Zhuqing Zhao, Matthias Wissuwa, Yoshinobu Takeuchi, Takeshi Ebitani, and Masahiro Yano. 2002. 'Response of rice to Al stress and identification of quantitative trait loci for Al tolerance', *Plant and Cell Physiology*, 43: 652-59.

Mapleson, Daniel, Gonzalo Garcia Accinelli, George Kettleborough, Jonathan Wright, and Bernardo J Clavijo. 2016. 'KAT: a K-mer analysis toolkit to quality control NGS datasets and genome assemblies', *Bioinformatics*, 33: 574-76.

Maron, Lyza G, Claudia T Guimarães, Matias Kirst, Patrice S Albert, James A Birchler, Peter J Bradbury, Edward S Buckler, Alison E Coluccio, Tatiana V Danilova, and David Kudrna. 2013. 'Aluminum tolerance in maize is associated with higher MATE1 gene copy number', *Proceedings of the National Academy of Sciences*, 110: 5241-46.

Martin, Marcel. 2011. 'Cutadapt removes adapter sequences from high-throughput sequencing reads', *EMBnet. journal*, 17: 10-12.

Melo, Janaina O, Ubiraci GP Lana, Miguel A Piñeros, Vera MC Alves, Claudia T Guimarães, Jiping Liu, Yi Zheng, Silin Zhong, Zhangjun Fei, and Lyza G Maron. 2013. 'Incomplete transfer of accessory loci influencing S b MATE expression underlies genetic background effects for aluminum tolerance in sorghum', *The Plant Journal*, 73: 276-88.

Minella, Euclydes, and Mark E Sorrells. 1992. 'Aluminum tolerance in barley: genetic relationships among genotypes of diverse origin', *Crop Science*, 32: 593-98.

bioRxiv preprint doi: https://doi.org/10.1101/843870; this version posted November 17, 2019. The copyright holder for this preprint (which was not certified by peer review) is the author/funder, who has granted bioRxiv a license to display the preprint in perpetuity. It is made available under aCC-BY-ND 4.0 International license.

867 Pertea, Mihaela, Geo M Pertea, Corina M Antonescu, Tsung-Cheng Chang, Joshua T
868 Mendell, and Steven L Salzberg. 2015. 'StringTie enables improved reconstruction of
869 a transcriptome from RNA-seq reads', *Nature biotechnology*, 33: 290.
870 Pizarro, Esteban A, Michael D Hare, Mpenzi Mutimura, and Bai Changjun. 2013. 'Brachiaria
871 hybrids: potential, forage use and seed yield', *Tropical Grasslands-Forrajes*
872 *Tropicales*, 1: 31-35.
873 Poschenrieder, Charlotte, Benet Gunsé, Isabel Corrales, and Juan Barceló. 2008. 'A glance
874 into aluminum toxicity and resistance in plants', *Science of the total environment*,
875 400: 356-68.
876 Powell, Sean, Kristoffer Forslund, Damian Szklarczyk, Kalliopi Trachana, Alexander Roth,
877 Jaime Huerta-Cepas, Toni Gabaldon, Thomas Rattei, Chris Creevey, and Michael
878 Kuhn. 2014. 'eggNOG v4. 0: nested orthology inference across 3686 organisms',
879 *Nucleic acids research*, 42: D231-D39.
880 Raman, Harsh, Kerong Zhang, Mehmet Cakir, Rudi Appels, David F Garvin, Lyza G Maron,
881 Leon V Kochian, J Sergio Moroni, Rosy Raman, and Muhammad Imtiaz. 2005.
882 'Molecular characterization and mapping of ALMT1, the aluminium-tolerance gene of
883 bread wheat (Triticum aestivum L.)', *Genome*, 48: 781-91.
884 Rao, Idupulapati M, John W Miles, Stephen E Beebe, and Walter J Horst. 2016. 'Root
885 adaptations to soils with low fertility and aluminium toxicity', *Annals of Botany*, 118:
886 593-605.
887 Roselló, Maite, Charlotte Poschenrieder, Benet Gunse, Juan Barceló, and Mercè Llugany.
888 2015. 'Differential activation of genes related to aluminium tolerance in two
889 contrasting rice cultivars', *Journal of inorganic biochemistry*, 152: 160-66.
890 Ryan, Peter R, Harsh Raman, Sanjay Gupta, Walter J Horst, and Emmanuel Delhaize.
891 2009. 'A second mechanism for aluminum resistance in wheat relies on the
892 constitutive efflux of citrate from roots', *Plant physiology*, 149: 340-51.
893 Salgado, Leonardo Rippel, Rodolpho Lima, Bruno Ferreira dos Santos, Karina Tamie
894 Shirakawa, Mariane de Almeida Vilela, Nalvo Franco Almeida, Rodrigo Matheus
895 Pereira, Alexandre Lima Nepomuceno, and Lucimara Chiari. 2017. 'De novo RNA
896 sequencing and analysis of the transcriptome of signalgrass (Urochloa decumbens)
897 roots exposed to aluminum', *Plant Growth Regulation*, 83: 157-70.
898 Schmutz, Jeremy, Phillip E McClean, Sujan Mamidi, G Albert Wu, Steven B Cannon, Jane
899 Grimwood, Jerry Jenkins, Shengqiang Shu, Qijian Song, and Carolina Chavarro.
900 2014. 'A reference genome for common bean and genome-wide analysis of dual
901 domestications', *Nature genetics*, 46: 707.

bioRxiv preprint doi: https://doi.org/10.1101/843870; this version posted November 17, 2019. The copyright holder for this preprint (which was not certified by peer review) is the author/funder, who has granted bioRxiv a license to display the preprint in perpetuity. It is made available under aCC-BY-ND 4.0 International license.

902 Simão, Felipe A, Robert M Waterhouse, Panagiotis Ioannidis, Evgenia V Kriventseva, and
903 Evgeny M Zdobnov. 2015. 'BUSCO: assessing genome assembly and annotation
904 completeness with single-copy orthologs', *Bioinformatics*, 31: 3210-12.
905 Simioni, Carine, and Cacilda Borges do Valle. 2009. 'Chromosome duplication in Brachiaria
906 (A. Rich.) Stapf allows intraspecific crosses', *Crop Breeding & Applied Biotechnology*,
907 9.
908 Smit, Arian FA, and Robert Hubley. 2008. 'RepeatModeler Open-1.0', *Available fom*
909 *http://www. repeatmasker. org*.
910 Stanke, Mario, Oliver Keller, Irfan Gunduz, Alec Hayes, Stephan Waack, and Burkhard
911 Morgenstern. 2006. 'AUGUSTUS: ab initio prediction of alternative transcripts',
912 *Nucleic acids research*, 34: W435-W39.
913 Tamura, Koichiro, Glen Stecher, Daniel Peterson, Alan Filipski, and Sudhir Kumar. 2013.
914 'MEGA6: molecular evolutionary genetics analysis version 6.0', *Molecular biology*
915 *and evolution*, 30: 2725-29.
916 Tanaka, Nobuhiro, Shimpei Uraguchi, Masataka Kajikawa, Akihiro Saito, Yoshihiro Ohmori,
917 and Toru Fujiwara. 2018. 'A rice PHD-finger protein Os TITANIA, is a growth
918 regulator that functions through elevating expression of transporter genes for multiple
919 metals', *The Plant Journal*, 96: 997-1006.
920 Tang, Y, David F Garvin, LV Kochian, ME Sorrells, and Brett F Carver. 2002. 'Physiological
921 genetics of aluminum tolerance in the wheat cultivar Atlas 66', *Crop Science*, 42:
922 1541-46.
923 Tarailo-Graovac, Maja, and Nansheng Chen. 2009. 'Using RepeatMasker to identify
924 repetitive elements in genomic sequences', *Current protocols in bioinformatics*, 25:
925 4.10. 1-4.10. 14.
926 Torkamaneh, Davoud, Jérôme Laroche, Maxime Bastien, Amina Abed, and François Belzile.
927 2017. 'Fast-GBS: a new pipeline for the efficient and highly accurate calling of SNPs
928 from genotyping-by-sequencing data', *BMC bioinformatics*, 18: 5.
929 Trapnell, Cole, Adam Roberts, Loyal Goff, Geo Pertea, Daehwan Kim, David R Kelley,
930 Harold Pimentel, Steven L Salzberg, John L Rinn, and Lior Pachter. 2012.
931 'Differential gene and transcript expression analysis of RNA-seq experiments with
932 TopHat and Cufflinks', *Nature protocols*, 7: 562.
933 Uga, Yusaku, Kazuhiko Sugimoto, Satoshi Ogawa, Jagadish Rane, Manabu Ishitani, Naho
934 Hara, Yuka Kitomi, Yoshiaki Inukai, Kazuko Ono, and Noriko Kanno. 2013. 'Control
935 of root system architecture by DEEPER ROOTING 1 increases rice yield under
936 drought conditions', *Nature genetics*, 45: 1097.

bioRxiv preprint doi: https://doi.org/10.1101/843870; this version posted November 17, 2019. The copyright holder for this preprint (which was not certified by peer review) is the author/funder, who has granted bioRxiv a license to display the preprint in perpetuity. It is made available under aCC-BY-ND 4.0 International license.

937 Valle, Cacilda Borges do, and Yves H Savidan. 1996. 'Genetics, cytogenetics, and
938 reproductive biology of Brachiaria.' in (Centro Internacional de Agricultura Tropical
939 (CIAT)).
940 Van der Auwera, Geraldine A, Mauricio O Carneiro, Christopher Hartl, Ryan Poplin,
941 Guillermo Del Angel, Ami Levy-Moonshine, Tadeusz Jordan, Khalid Shakir, David
942 Roazen, and Joel Thibault. 2013. 'From FastQ data to high-confidence variant calls:
943 the genome analysis toolkit best practices pipeline', *Current protocols in*
944 *bioinformatics*, 43: 11.10. 1-11.10. 33.
945 Venturini, Luca, Shabhonam Caim, Gemy George Kaithakottil, Daniel Lee Mapleson, and
946 David Swarbreck. 2018. 'Leveraging multiple transcriptome assembly methods for
947 improved gene structure annotation', *GigaScience*, 7: giy093.
948 Von Uexküll, HR, and E Mutert. 1995. 'Global extent, development and economic impact of
949 acid soils', *Plant and soil*, 171: 1-15.
950 Wenzl, Peter, Adriana Arango, Alba L Chaves, Maria E Buitrago, Gloria M Patino, John
951 Miles, and Idupulapati M Rao. 2006. 'A greenhouse method to screen
952 brachiariagrass genotypes for aluminum resistance and root vigor', *Crop Science*, 46:
953 968-73.
954 Wenzl, Peter, Gloria M Patino, Alba L Chaves, Jorge E Mayer, and Idupulapati M Rao. 2001.
955 'The high level of aluminum resistance in signalgrass is not associated with known
956 mechanisms of external aluminum detoxification in root apices', *Plant physiology*,
957 125: 1473-84.
958 Wickham, Hadley, and Winston Chang. 2008. 'ggplot2: An implementation of the Grammar
959 of Graphics', *R package version 0.7, URL: http://CRAN. R-project. org/package=*
960 *ggplot2*, 3.
961 Worthington, M, Masumi Ebina, Naoki Yamanaka, Christopher Heffelfinger, Constanza
962 Quintero, Yeny Patricia Zapata, Juan Guillermo Perez, Michael Selvaraj, Manabu
963 Ishitani, and Jorge Duitama. 2019. 'Translocation of a parthenogenesis gene
964 candidate to an alternate carrier chromosome in apomictic Brachiaria humidicola',
965 *BMC genomics*, 20: 41.
966 Worthington, M, Christopher Heffelfinger, Diana Bernal, Constanza Quintero, Yeny Patricia
967 Zapata, Juan Guillermo Perez, Jose De Vega, John Miles, Stephen Dellaporta, and
968 Joe Tohme. 2016. 'A parthenogenesis gene candidate and evidence for segmental
969 allopolyploidy in apomictic Brachiaria decumbens', *Genetics*, 203: 1117-32.
970 Worthington, ML, and John W Miles. 2015. 'Reciprocal full-sib recurrent selection and tools
971 for accelerating genetic gain in apomictic Brachiaria.' in, *Molecular breeding of forage*
972 *and turf* (Springer).

bioRxiv preprint doi: https://doi.org/10.1101/843870; this version posted November 17, 2019. The copyright holder for this preprint (which was not certified by peer review) is the author/funder, who has granted bioRxiv a license to display the preprint in perpetuity. It is made available under aCC-BY-ND 4.0 International license.

973 Wu, Thomas D, Jens Reeder, Michael Lawrence, Gabe Becker, and Matthew J Brauer.
974 2016. 'GMAP and GSNAP for genomic sequence alignment: enhancements to
975 speed, accuracy, and functionality.' in, *Statistical Genomics* (Springer).
976 Xia, Jixing, Naoki Yamaji, Tomonari Kasai, and Jian Feng Ma. 2010. 'Plasma membrane-
977 localized transporter for aluminum in rice', *Proceedings of the National Academy of*
978 *Sciences*, 107: 18381-85.
979 Yamaji, Naoki, Chao Feng Huang, Sakiko Nagao, Masahiro Yano, Yutaka Sato, Yoshiaki
980 Nagamura, and Jian Feng Ma. 2009. 'A zinc finger transcription factor ART1
981 regulates multiple genes implicated in aluminum tolerance in rice', *The Plant Cell*, 21:
982 3339-49.
983 Yang, Jian Li, Xiao Fang Zhu, You Xiang Peng, Cheng Zheng, Gui Xin Li, Yu Liu, Yuan Zhi
984 Shi, and Shao Jian Zheng. 2011. 'Cell wall hemicellulose contributes significantly to
985 aluminum adsorption and root growth in Arabidopsis', *Plant physiology*, 155: 1885-
986 92.
987 Yokosho, Kengo, Naoki Yamaji, and Jian Feng Ma. 2011. 'An Al-inducible MATE gene is
988 involved in external detoxification of Al in rice', *The Plant Journal*, 68: 1061-69.
989 Zhang, Gengyun, Xin Liu, Zhiwu Quan, Shifeng Cheng, Xun Xu, Shengkai Pan, Min Xie,
990 Peng Zeng, Zhen Yue, and Wenliang Wang. 2012. 'Genome sequence of foxtail
991 millet (Setaria italica) provides insights into grass evolution and biofuel potential',
992 *Nature biotechnology*, 30: 549.
993

bioRxiv preprint doi: https://doi.org/10.1101/843870; this version posted November 17, 2019. The copyright holder for this preprint (which was not certified by peer review) is the author/funder, who has granted bioRxiv a license to display the preprint in perpetuity. It is made available under aCC-BY-ND 4.0 International license.

994 **Figure 1:** Root growth in *B. decumbens* accession CIAT606 and *B. ruziziensis* accession
995 BRX4404 after growing for 20 days in control and high 200 µM Al^{3+} concentration hydroponic
996 solutions.

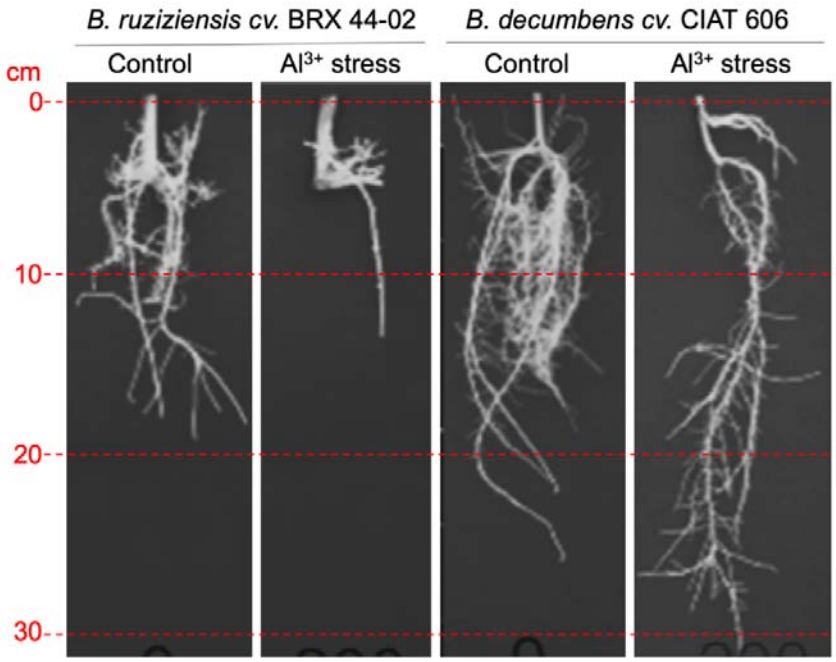

997
998

bioRxiv preprint doi: https://doi.org/10.1101/843870; this version posted November 17, 2019. The copyright holder for this preprint (which was not certified by peer review) is the author/funder, who has granted bioRxiv a license to display the preprint in perpetuity. It is made available under aCC-BY-ND 4.0 International license.

Figure 2: Root length (RL), root biomass (RB), and root tip diameter (RD) ratios between Al^{3+} stress and control measured values (stress/control) in the interspecific progeny between *B. ruziziensis* and *B. decumbens* (n=169).

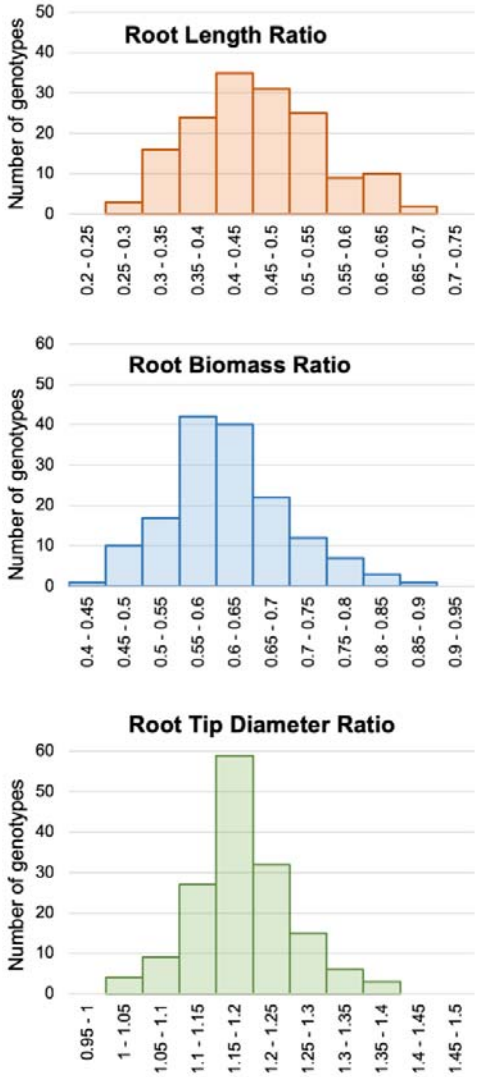

bioRxiv preprint doi: https://doi.org/10.1101/843870; this version posted November 17, 2019. The copyright holder for this preprint (which was not certified by peer review) is the author/funder, who has granted bioRxiv a license to display the preprint in perpetuity. It is made available under aCC-BY-ND 4.0 International license.

1003 **Figure 3:** Synteny between the *Brachiaria ruziziensis* and *Setaria italica* genomes. The 36
1004 synteny blocks longer than 1 Mbp and the translocation are highlighted in red or green
1005 boxes according to their direction.

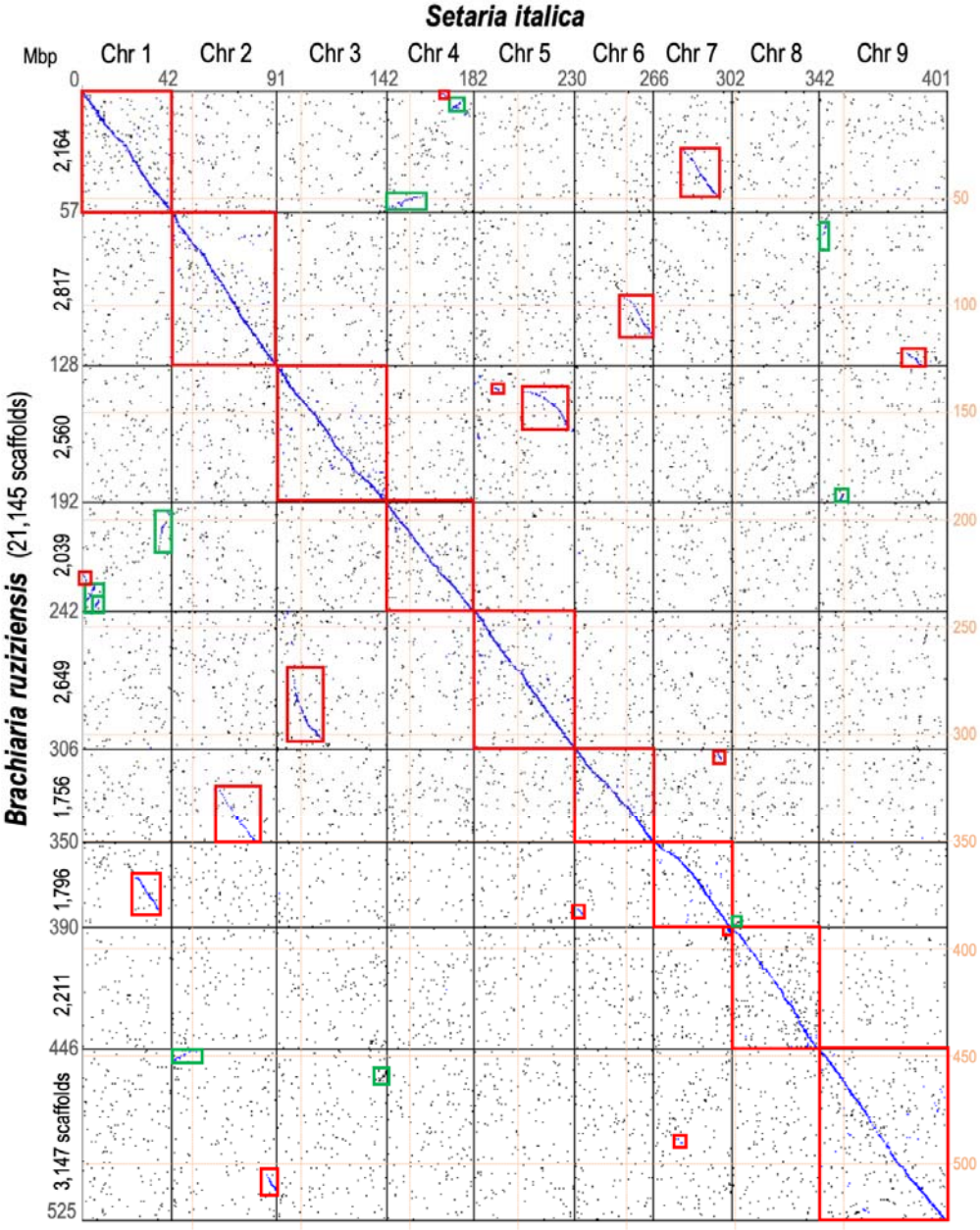

1006
1007
1008

bioRxiv preprint doi: https://doi.org/10.1101/843870; this version posted November 17, 2019. The copyright holder for this preprint (which was not certified by peer review) is the author/funder, who has granted bioRxiv a license to display the preprint in perpetuity. It is made available under aCC-BY-ND 4.0 International license.

Figure 4: 4,427 genetic markers placed in 18 linkage groups. We defined three QTLs each in LG 1 (Chr 8) for root length and biomass, LG 3 (Chr 7) for root length, and LG 4 (Chr 3) for root diameter. As a control, the apomictic locus was identified from reproductive mode phenotyping.

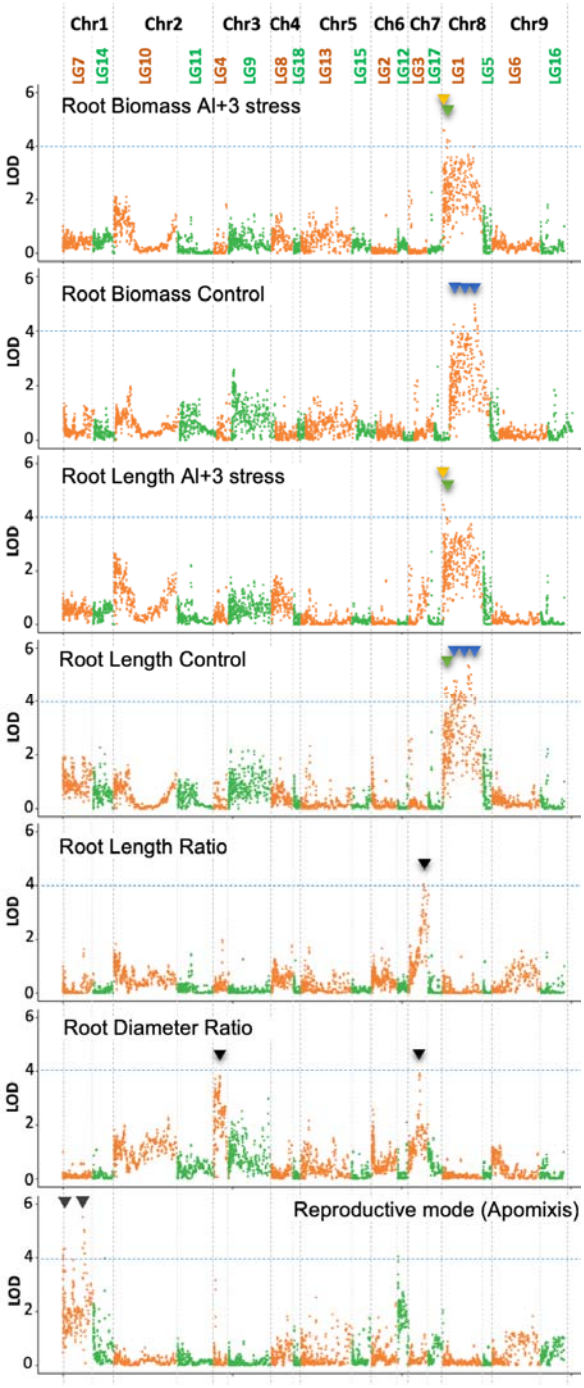

bioRxiv preprint doi: https://doi.org/10.1101/843870; this version posted November 17, 2019. The copyright holder for this preprint (which was not certified by peer review) is the author/funder, who has granted bioRxiv a license to display the preprint in perpetuity. It is made available under aCC-BY-ND 4.0 International license.

1014 **Figure 5:** Differentially expressed (DE) genes in roots from the three accessions with
1015 different levels of tolerance to high (200 µM $AlCl^3$) aluminium cation concentrations.

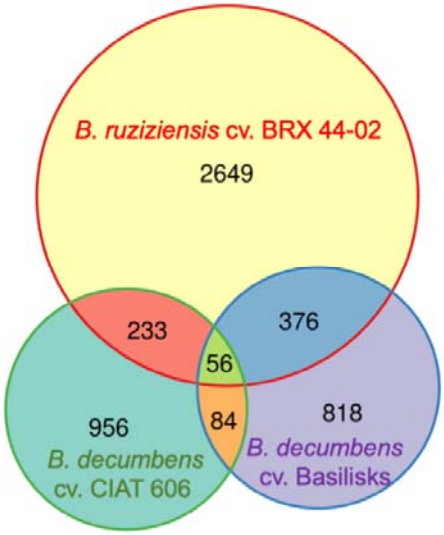

1016
1017

bioRxiv preprint doi: https://doi.org/10.1101/843870; this version posted November 17, 2019. The copyright holder for this preprint (which was not certified by peer review) is the author/funder, who has granted bioRxiv a license to display the preprint in perpetuity. It is made available under aCC-BY-ND 4.0 International license.

Figure 6: Bubble plot of enriched GO terms. Each bubble represents an overrepresented GO slim terms, in red if it is overrepresented among DE upregulated genes or in blue if among downregulated ones. The size is proportional to the number of DE genes that support that enrichment. The intensity of colour is proportional to the Pval of the enrichment test (Fisher test). Brachiaria species are sorted left to right from high to low aluminium-tolerance: Basi (*B. decumbens* cv. Basilisks), Bdec (*B. decumbens* cv. CIAT 606, Bruz (*B. ruziziensis* cv. BRX 44-02).

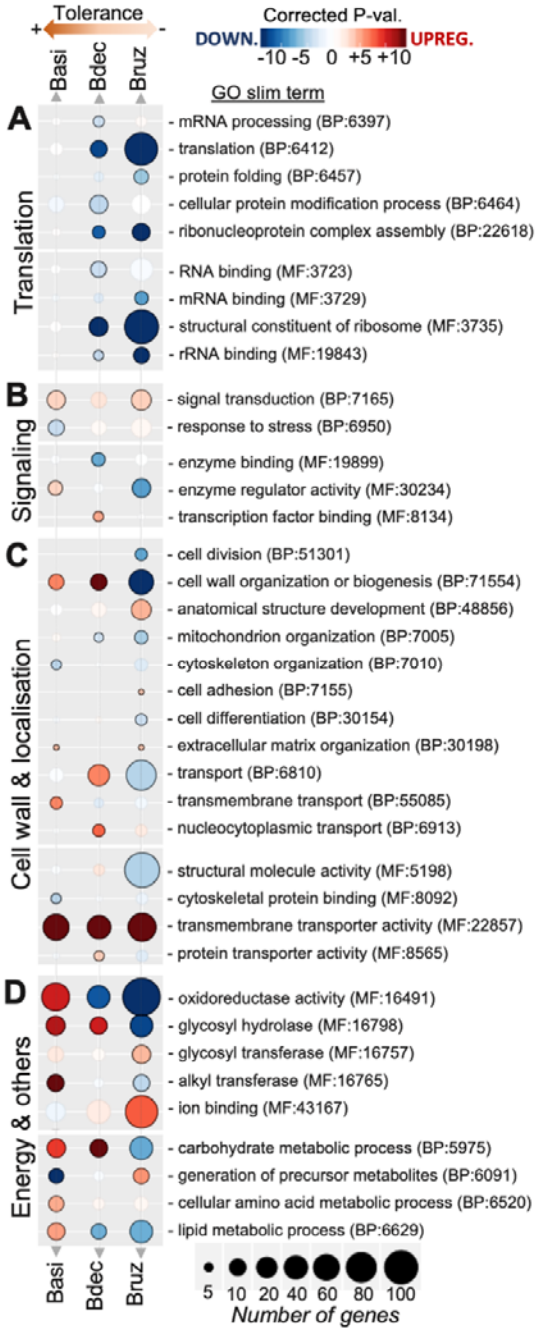

bioRxiv preprint doi: https://doi.org/10.1101/843870; this version posted November 17, 2019. The copyright holder for this preprint (which was not certified by peer review) is the author/funder, who has granted bioRxiv a license to display the preprint in perpetuity. It is made available under aCC-BY-ND 4.0 International license.

1028 **Table 1:** Statistics associated with the assembly of the *Brachiaria ruziziensis* reference
1029 genome and anchored in pseudo-molecules..

	Whole genome assembly (WGA)	**Pruned WGA***	**Anchored assembly**
Total length	732.5 Mbp	533.9 Mbp	525.1 Mbp
% Ns	10.6 %	11.7 %	12.18 %
Number sequences	102,579	23,076	7 pseudo-chrs
N50	27.8 Kbp	44.6 Kbp	55.9 Mbp
N20	76.1 Kbp	91.7 Kbp	62.7 Mbp
N80	3.9 Kbp	19.5 Kbp	44.1 Mbp

1030 WGA deposited in NCBI, accession number GCA_003016355. Anchoring available in AGP
1031 format, together with the raw reads, in the Bioproject PRJNA437375. *Sequences without
1032 genes and under 10Kbp have been removed.

1033 **Table 2:** *Brachiaria* genes differentially expressed during Al^{3+} stress, homologous to Al-induced proteins or related Gene Ontology (GO) terms.

GENE	Bruz	Bdec	Basi	Gene name	Uniprot	P. halli	S. itallica	S. viridis	A. thaliana	Function and induction
29G2	0.71	**0.17**	-0.18	STOP1	STOP1_ORYSJ	3G044400	7G287100	7G299300	AT1G34370	Zinc-finger Transcription factor involved in aluminium tolerance
61G2	0.88	**0.23**	0.07	Citrate transporter detoxification 42	DTX42_ARATH	9G552400	9G489200	9G493200	AT1G51340	Citrate transporter responsible for citrate exudation into the rhizosphere to protect roots from aluminium toxicity. Upregulated by aluminium. Expressed in roots, but not in shoots.
122G16	**1.58**	**1.62**	0.01	Nitrate reductase	NIA3_MAIZE	6G233200	6G178500	6G184900	AT1G77760	Nitrate reductase
126G26	**1.83**	**0.95**	-0.11	STOP1	STOP1_ORYSJ	6G306100	6G252000	6G256600	AT5G22890	Transcription factor involved in aluminium tolerance
211G30	-0.20	0.00	**-0.81**	Tonoplast dicarboxylate	TDT_ARATH	2G311500	2G251700	2G262500	AT5G47560	Carrier involved in the uptake of malate and fumarate to the vacuole. Inhibited by citrate. Critical for pH homeostasis. Induced by malate and by acidification of the cytoplasm.
211G34	-0.01	0.06	**-0.80**	Tonoplast dicarboxylate	TDT_ARATH	2G311400	2G251700	2G262500	AT5G47560	Carrier involved in the uptake of malate and fumarate to the vacuole. Inhibited by citrate. Critical for pH homeostasis. Induced by malate and by acidification of the cytoplasm.
259G14	**2.36**	**1.43**	0.10	Citrate transporter protein detox. 42	DTX42_ARATH	9G201000	9G204700	9G203100	AT1G51340	Citrate transporter responsible for citrate exudation into the rhizosphere to protect roots from aluminium toxicity. Upregulated by aluminium. Expressed in roots, but not in shoots.
462G24	-2.35	**0.38**	0.01	AMLT10	K3XVN8_SETIT	4G147500	4G162600	4G130000		Aluminium-activated malate transporter 10-like
675G12	**4.27**	**3.89**	0.01	Citrate transporter protein detox. 42	DTX42_ARATH	5G042400	9G489200	9G493200	AT1G51340	Citrate transporter responsible for citrate exudation into the rhizosphere to protect roots from aluminium toxicity. Upregulated by aluminium. Expressed in roots, but not in shoots.
1615G2	**2.69**	**1.29**	0.01	STOP1	STOP1_ORYSJ	6G306100	6G252000	6G256600	AT5G22890	Zinc-finger Transcription factor involved in aluminium tolerance
1766G4	**1.34**	**0.96**	**-0.24**	MST3	MST3_ORYSJ	2G004500	2G000400	2G004300	AT3G19930	Involved in the accumulation of monosaccharides required for cell wall synthesis during root development. Highly expressed in in xylem and sclerenchyma cells of roots.
1984G2	1.09	**0.82**	0.09	SLK2	SLK2_ARATH	4G345700	4G015400	4G015300	AT5G62090	DNA-binding adapter subunit of the SEU-SLK2 transcriptional corepressor of abiotic stress (e.g. salt and osmotic stress) response genes by facilitating auxin response and sustaining meristematic potential.
2499G8	1.18	**-0.15**	0.03	OsTITANIA/AtOBE3	TTA1_ORYSJ	9G552000	9G488800	9G492800	AT1G14740	Widely expressed transcription factor that functions as regulator of metal transporter genes responsible for essential metals delivery to shoots and normal plant growth. Required for the maintenance of metal transporter gene expression, such as IRT1, IRT2, ZIP1, ZIP9, NRAMP1 and NRAMP5.
2708G4	**1.64**	**1.94**	**0.42**	Auxin transport protein BIG	BIG_ORYSJ	2G178200	2G154800	2G160200	AT3G02260	Auxin-mediated developmental responses (e.g. cell elongation, apical dominance, lateral root production, inflorescence architecture, general growth and development).
3096G6	0.51	**0.27**	-0.04	ALS1	AB25B_ORYSJ	9G083700	9G088000	9G086400	AT5G39040	Metal transporter involved in the sequestration of aluminium into vacuoles, which is required for cellular detoxification of aluminium. Induced by aluminium in roots. Expressed in primary roots and lateral roots.
3672G6	**2.54**	**2.26**	-0.16	NRAT1	NRAT1_ORYSJ	1G025100	1G098100	1G097200	AT1G80830	Metal transporter Al3+, but not divalent cations Fe2+, Mg2+, Cd2+. Involved in Al tolerance by taking up Al in root cells, where it is detoxified by chelation with organic acid anions and sequestration into the vacuoles. Induced by aluminium in roots. Positively regulated by ART1.
4534G2	**4.74**	**0.43**	0.08	SAD2 importin beta-like transporter	SAD2_ARATH	7G101600	7G051600	7G057300	AT2G31660	Involved in the regulation of the abscisic acid (ABA)-mediated pathway in response to cold or salt stress, UV-B responses. Involved in trichome initiation. Negative regulator miRNA activity. Expressed in roots, epidermal and guard cells of leaves, stems and siliques
5233G2	**1.07**	**1.18**	-0.19	XTH23	XTH23_ARATH	4G029300	4G246200	4G258800	AT4G25810	Xyloglucan endotransglucosylase hydrolase protein 23 cleaves and religates xyloglucan polymers, an essential constituent of the primary cell wall, and thereby participates in cell wall construction of growing tissues. Upregulated by abscisic acid (ABA).
5400G2	-1.38	**-0.05**	0.08	XTH	XTH5_ARATH	8G197800	8G142000	8G151900	AT5G13870	Cleaves and religates xyloglucan polymers, an essential constituent of the primary cell wall, and thereby participates in cell wall construction of growing tissues. Strongly down regulated by abscisic acid. Root specific.
6544G2	**-0.07**	0.95	-0.04	XTH32	XTH8_ORYSJ	2G372300	2G313800	2G324800	AT2G36870	Xyloglucan endotransglucosylase hydrolase protein 32 cleaves and religates xyloglucan polymers, an essential constituent of the primary cell wall, and thereby participates in cell wall construction of growing tissues. May be involved in cell elongation processes. Induced by gibberellic acid (GA3).
6944G2	**1.92**	**2.01**	0.02	Phospholipid transporting ATPase	ALA12_ARATH	4G247400	4G147300	4G165700	AT1G26130	Involved in transport of phospholipids.
7361G2	**2.26**	**1.39**	0.00	STAR2/ALS3	STAR2_ORYSJ	3G099200	3G043600	3G044400	AT2G37330	Associates with STAR2 to form a functional transmembrane ABC transporter required for detoxification of aluminium (Al) in roots. Can specifically transport UDP-glucose. Induced by Al in roots. Positively regulated by ART1. Root specific.
7811G2	**-0.68**	**0.86**	0.06	Germin-like protein 5-1	GL52_ORYSJ	5G433600	5G062400	5G061900	AT3G62020	Manganese metal-binding intracellular transporter involved in root development. May play a role in plant defense. Probably has no oxalate oxidase activity.
8068G4	**2.77**	**2.12**	0.01	Mg transporter MRS2-D	MRS2D_ORYSJ	7G150800	7G099600	7G107500	AT3G19640	Putative magnesium transporter.
8448G4	**0.59**	**1.26**	**-0.24**	STAR1	STAR1_ORYSJ	4G029500	4G246800	4G259400	AT1G67940	Associates with STAR2 to form a functional transmembrane ABC transporter required for detoxification of aluminium (Al) in roots. Can specifically transport UDP-glucose. Induced by Al in roots. Positively regulated by ART1. Root specific.
11634G4	**0.04**	4.75	-0.01	AMLT1	ALMT8_ARATH	7G143300	7G007400	7G102000	AT3G11680	Malate transporter.
11683G4	1.00	**0.66**	0.00	XTH27	A0A1D6K9K3_ZM					Xyloglucan endotransglucosylase hydrolase protein 27 cleaves and religates xyloglucan polymers, an essential constituent of the primary cell wall, and thereby participates in cell wall construction of growing tissues.
12087G2	**1.31**	**3.21**	-0.03	Phosphate transporter pho1-2	PHO12_ORYSJ	1G440700	1G360400	1G367100	AT3G23430	Involved in the transfer of inorganic phosphate (Pi) from roots to shoots. Not induced by Pi deficiency in roots. Specifically expressed in roots.
14972G2	**-0.56**	**0.96**	0.13	GTP-binding nuclear protein RAN2	RAN2_ORYSJ	5G226400	5G244500	5G252400	AT5G20010	GTP-binding protein involved in nucleocytoplasmic transport. Required for the import of protein into the nucleus and also for RNA export. Involved in chromatin condensation and control of cell cycle.
26018G2	**1.08**	**0.98**	**-0.22**	transporter NRT1 nitrate transporter	PTR27_ARATH	9G390400	9G327900	9G333900	AT2G26690	Low-affinity proton-dependent nitrate transporter. Upregulated in the shoots by nitrate, but no changes in the roots.
30107G2	**3.24**	3.02	-0.01	NRAT1	NRAT1_ORYSJ	2G074500	1G098100	1G097200	AT1G80830	Metal transporter Al3+, but not divalent cations Fe2+, Mg2+, Cd2+. Involved in Al tolerance by taking up Al in root cells, where it is detoxified by chelation with organic acid anions and sequestration into the vacuoles. Induced by aluminium in roots. Positively regulated by ART1.
87018G2	**3.19**	**2.16**	-0.05	ABC transporter C family member 9	AB4C_MAIZE	7G270200	7G216700	7G228400	AT3G60160	ABC transporter that may affect phytic acid transport and compartmentalization. May function directly or indirectly in removing phytic acid from the cytosol or in vesicle trafficking. Expressed in roots, leaves, stalks, tassels, silks, developing seeds and embryos.
89122G2	**3.41**	**1.40**	0.02	ABC transporter C family member 15	AB4C_MAIZE	7G270200	7G216700	7G228400	AT3G60160	ABC transporter that may affect phytic acid transport and compartmentalization. May function directly or indirectly in removing phytic acid from the cytosol or in vesicle trafficking. Expressed in roots, leaves, stalks, tassels, silks, developing seeds and embryos.

bioRxiv preprint doi: https://doi.org/10.1101/843870; this version posted November 17, 2019. The copyright holder for this preprint (which was not certified by peer review) is the author/funder, who has granted bioRxiv a license to display the preprint in perpetuity. It is made available under aCC-BY-ND 4.0 International license.

bioRxiv preprint doi: https://doi.org/10.1101/843870; this version posted November 17, 2019. The copyright holder for this preprint (which was not certified by peer review) is the author/funder, who has granted bioRxiv a license to display the preprint in perpetuity. It is made available under aCC-BY-ND 4.0 International license.